The phytoliths of Naachtun (Petén, Guatemala): Development of a modern reference for the characterization of plant communities in the Maya Tropical Lowlands

Marc Testé, Aline Garnier, Nicole Limondin-Lozouet, Enecon Oxlaj, Cyril Castanet, Louise Purdue, Eva Lemonnier, Lydie Dussol, Philippe Nondédéo

Abstract:

Phytoliths, unlike pollen and charcoal, are frequently conserved in sediments in the Maya lowlands but are rarely used as paleoenvironmental proxies. To better interpret and reconstruct paleoecological signatures and changes, it is necessary to provide current analogues of fossil assemblages. To do so, we selected six modern ecosystems and differentiated them by their soil phytolith assemblages in the ancient Maya city of Naachtun (northern Petén, Guatemala). We studied the plant communities and relative phytoliths frequencies in surface soils on four north-south vegetation transect, composed of 43 quadrats. These transects cross forests and savannahs in low swampy areas North and South of the site, and hill forest in its center, where the city was built. Quadrats were statistically compared using multivariate analyses (CA). Six types of plant communities were characterized by their phytolith assemblages, as well as on the presence of siliceous bioindicators such as diatoms and sponges. The D/P and LU indexes developed for these assemblages allow us to provide a precise signature of the current vegetation cover, and identify the presence of undergrowth in forest areas, or forest edges in savannah areas. This first modern phytolith reference for the Maya area will contribute to the development of paleoecological reconstructions for this zone.

The phytoliths of Naachtun (Petén, Guatemala): Development of a modern reference for the characterization of plant communities in the Maya Tropical Lowlands

Marc Testé [a,b,*], Aline Garnier [c,a], Nicole Limondin-Lozouet [a], Enecon Oxlaj [d], Cyril Castanet [e,a], Louise Purdue [f], Eva Lemonnier [b,g], Lydie Dussol [f,g], Philippe Nondédéo [g]

[a] Laboratoire de Géographie Physique, LGP CNRS-UMR8591, 1 place Aristide Briand, 92195 Meudon, France

[b] Université Paris 1 Panthéon-Sorbonne, 191 rue Saint Jacques, 75005 Paris, France

[c] Université de Paris Est Créteil - Val de Marne, 61 avenue du Général de Gaulle, 94010 Créteil, France

[d] Organización de Manejo y Conservación, OMYC, Uaxactún, Petén, Guatemala

[e] Université Paris 8 Vincennes - Saint Denis, 2 Rue de la Liberté, 93526 Saint-Denis

[f] Université Côte d'Azur, CNRS, CEPAM, Pôle Universitaire Saint Jean d'Angély SJA 3, 24, avenue des Diables Bleus, 06357 Nice Cedex 4, France

[g] CNRS, Archéologie des Amériques, Maison Archéologie Ethnologie, 21, allée de l'Université, 92023 Nanterre, France

[*] Corresponding author: marc.teste@lgp.cnrs.fr

Highlights

- Botanical description of 6 plant communities in the Petén
- Distinction and identification of ecosystems through phytolith assemblages
- Use of phytolith indices to specify the ecology of plant formations
- First modern environmental reference for phytoliths in the Maya lowlands

Abstract

Phytoliths, unlike pollen and charcoal, are frequently conserved in sediments in the Maya lowlands but are rarely used as paleoenvironmental proxies. To better interpret and reconstruct paleoecological signatures and changes, it is necessary to provide current analogues of fossil assemblages. To do so, we selected six modern ecosystems and differentiated them by their soil phytolith assemblages in the ancient Maya city of Naachtun (northern Petén, Guatemala). We studied the plant communities and relative phytoliths frequencies in surface soils on four north-south vegetation transect, composed of 43 quadrats. These transects cross forests and savannahs in low swampy areas North and South of the site, and hill forest in its center, where the city was built. Quadrats were statistically compared using multivariate analyses (CA). Six types of plant communities were characterized by their phytolith assemblages, as well as on the presence of siliceous bioindicators such as diatoms and sponges. The D/P and LU indexes developed for these assemblages allow us to provide a precise signature of the current vegetation cover, and identify the presence of undergrowth in forest areas, or forest edges in savannah areas. This first modern phytolith reference for the Maya area will contribute to the development of paleoecological reconstructions for this zone.

Keywords

Phytoliths assemblages; Naachtun; Maya Lowland, Petén forests; *Sival* wetland; phytolith indexes

1. Introduction

Today, while more and more studies are focusing on the systemic collapse of our modern civilization (Meadows et al., 2004; Erhlich and Ehrlich, 2013; Servigne and Stevens, 2015), some are interested in ancient societies that have disappeared as a way of addressing modern social or

environmental crises (Tainter, 1988; Diamond, 2005). The Maya societies of the Yucatán Lowland, well known for their huge architectural remains, are a good example. Studies testify to two major collapse events that occurred in the 2nd century (pre-classical collapse) and the 10th century (classical collapse) CE. While these collapse events are sometimes presented as the result of overly intensive environmental exploitation (Abrams and Rue, 1988; Hansen et al. 2002; Lentz and Hockaday, 2009; Turner and Sabloff, 2012), other authors question this hypothesis by citing the Maya's considered and sustainable management of forest and plant resources (Fedick, 2010; Mcneil, 2012; Lentz et al., 2015; Thompson et al., 2015).

Located in the extreme north of Guatemala (Fig. 1), four kilometers from the border with Campeche (Mexico), the archaeological site of Naachtun was first surveyed in 1922, by SG. Morley, and 10 years later by CL. Lundell (Lundell, 1932). Since 2000, Naachtun has been the site of archaeological and palaeoenvironmental studies (Reese-Taylor et al., 2005; Nondédéo et al., 2012; 2013) and is also one of the location of the Lidar project, which aims to map the geographical and archaeological characteristics of Maya sites in northern Guatemala (Canuto et al., 2018). Given its well-preserved monumental remains, the site holds a certain archaeological interest. Indeed, the first archaeological evidence of occupation dates to the 5th century BCE, although the development of the city only began in earnest in the 1st century CE; that is, at around the time of the pre-classical period Maya collapse (Hansen et al., 2002). Located halfway between Tikal and Calakmul, the two great Maya kingdoms of Petén during the classical period, Naachtun played the role of a regional political center and may have counted several thousand inhabitants. The site was eventually abandoned around 950 CE, relatively late period in comparison to the other capitals of the Petén region (Nondédéo et al., 2013).

In order to understand the link between past cultural and environmental changes, this study uses both the archaeological context and geomorphological/palaeoenvironmental context. Naachtun is located on a large hilly escarp and is bordered to the north and south by two depressions of the karstic polje type (Castanet et al. 2016), called *bajos*, with dispersed perennial wetlands, locally called *Sival* (Fig. 2). During the wet season, these *Sival* are fed by water and result in considerable

palustrine-alluvial sedimentation. These sedimentary sequences located in the northern *bajo* cover the periods of occupation of the Naachtun site and create a good trap for the bioindicators (phytoliths, mollusks, etc.) used for palaeoenvironmental reconstructions.

In the Maya Lowlands, most bio-proxies used in palaeoenvironmental studies to reconstruct past vegetation dynamics are either pollen (Islebe, 1996; Leyden, 2002; Carozza et al., 2007; Wahl et al., 2006; 2013) or charcoal (Lentz and Hockabay, 2009; Lentz, 2015; Dussol et al., 2017). However, in Naachtun's *bajo* records, pollen are poorly preserved, while the identifiable charcoals are too diluted to allow for systematic study. This poor conservation led us to look for new bioindicators of past vegetation changes. Due to their siliceous structure, phytoliths are resistant to oxidation and are well preserved in such tropical environment deposits (Alexandre, et al., 1997; Madella and Lancelotti, 2012; Piperno, 2006; Watling et al., 2016). They also allow good monitoring of herbaceous environments thanks to the morphotype diversity of Cyperaceae and Poaceae (Twiss et al., 1969; Fredlund and Tieszen, 1994; Lu and Liu, 2003; Stromberg, 2004, Iriarte and Paz, 2009; Novello et al., 2012). Moreover, unlike pollen, phytoliths are a good local bioindicator of plant formations (Madella and Lancelotti, 2012; Piperno, 2006). However, in the Maya zone, research involving phytoliths is scarce and has been conducted using only a few particular morphotypes (Beach et al., 2009), or in specific archaeological contexts (Bozart and Guderjan, 2004; Abramiuk et al., 2011).

Given the lack of phytolith studies in this forest region, it is difficult to interpret fossil assemblages in the sedimentary archives. The main problem in forest environments is that phytoliths do not allow for taxonomic discrimination between woody dicotyledons (Alexandre et al., 1997; Piperno, 2006; Mercader et al., 2009; Collura and Neumann, 2017). However, in similar environments of tropical lowland forests, like the Amazon rainforest, recent studies have pointed to the possibility of characterizing the different forest ecosystems by studying phytolith assemblages (Dickau et al., 2013; Watling et al., 2016).

The aim of this study is, therefore, to assess the potential of phytoliths in the Maya Lowlands to serve as a good proxy of plant formations. To achieve this purpose, a botanical study

has been carried out on 43 ecological quadrats located along four transects crossing the different ecosystems of the Naachtun site. For each quadrat, surface soils were sampled and phytolith assemblages analyzed using the general counting and index approaches. The link between phytolith assemblages and plant communities was tested using a distribution diagram, and also a statistical study using a component analysis. In this paper, we will compare the different phytolith indexes and propose a new index to better establish the landscape characteristics of these communities.

2. Study Area

2.1. Climate and geology

The department of Petén is located in the southern part of the Petén tropical forest covering the central lowlands of the Yucatán peninsula, also referred as the Maya Lowlands (Fig. 1). The vegetation of Petén is mainly subject to two control factors: precipitations and regional geomorphology (Sánchez-Sánchez and Islebe, 2002; Carrilo-Bastos et al., 2012). Indeed, seasonal latitudinal migrations of the Inter-Tropical Convergence Zone (ITCZ) and the North Atlantic High cause considerable seasonality of precipitation (Hastenrath, 1976; 1984; Brenner et al., 2001; Hodell et al., 2005; Carrillo-Bastos et al., 2012). Thus, most of the rainfall, between 1,000 and 1,500 mm, is concentrated in the period from May to December, while the period from January to April corresponds to a dry season. Due to the intertropical position of the peninsula, temperatures remain relatively stable throughout the year (Wilson, 1980). These umbrothermal conditions correspond to an Am-type climate in the Köppen classification (Pennington and Sarukhán, 2005). The regional geomorphology of Petén is a vast Meso-Cenozoic carbonate platform, composed mainly of limestone, at low altitude (250–300 m). The fractures and heterogeneities of the limestone bedrock have produced karstified landscapes resulting in hills alternating with depressions (*bajos*) (Dunning et al., 2002; Beach et al., 2008, 2009). Consequently, differences in hydrology and soil

composition are also observed, with thin layers of well-drained rendosol on hill and slope areas, and seasonally waterlogged vertisol-histosol in *bajo* areas (Beach et al., 2008).

2.2. The plant formations of Petén

The Petén forest was first described in the 1930s by Lundell (1937) and was defined as a semi-sempervirent tropical forest. However, this ecological classification does not reflect the true diversity of forest ecosystems found in the different geomorphological contexts of Petén. The hill zones are covered by high semi-evergreen forests (30–40 m) with calcareous plant associations. The wide trees, characteristic of these forests, belong mostly to the Burseraceae, Fabaceae, Meliaceae, Moraceae, Sapindaceae, and Sapotaceae. The relatively sparse undergrowth is occupied by Arecaceae and Piperaceae shrubs, and a small number of grassy plants. The *bajo* areas are covered by a low forest (5–8 m), where plant associations are adapted to clayey soils and the seasonal submersions and drying periods. These are mainly composed of species belonging to the Anacardiaceae, Euphorbiaceae, Fabaceae and Myrtaceae families. The *bajo* forest undergrowth is relatively bare, with very few grasses. In addition to these two main forest ecosystems, it is possible to find other vegetation types, such as palm forests, pine forests, or humid or dry savannahs, adapted to local geomorphological conditions (Lundell, 1937; Martínez and Galindo-Leal, 2002; Schulze and Whitacre, 1999). Currently, the Petén forests are less populated than during the Maya period (Canuto et al., 2018).

3. Methodology

3.1. Vegetation study and soil sampling

The vegetation study was conducted during two fieldwork sessions at the end of the dry season in March 2016 and April 2017. We have conducted ecological transects crossing all altitude

and humidity domains. Thus, we defined three north-south oriented transects in the north *bajo* area (T1, T2, and T3), and one north-south/west oriented transect (T4), over distances of about one kilometer. These transects therefore covered different plant formations of forests and herbaceous areas from hills and *bajo* (Fig. 2). Along these transects, we identified areas where plant communities were changing. Depending on the extent of a plant community, one to two blocks, each of about 100m², have been positioned in the middle of it. On each quadrat, we recorded the plant species presences based on local common names and annotated their relative quantity. Vegetation cover values were estimated from colorimetric processing (light rate [light-white pixels] relative to vegetation coverage rate [dark pixels]) of forest cover photographs taken vertically and to up. Finally, for the phytolith analysis, only a few grams of the surface portion of the A1 horizon (the A0 litter having been removed from the sample) were taken from several locations in each of the quadrat. All samples were mixed to create a single sample of approximately 100 g by quadrat. It allowed us to prevent our sampling producing ultra-local biases in phytolith assemblages.

The ecological survey was carried out with the help of a local forester able to identify the plants by their vernacular names in Spanish and/or Mayan. The vernacular names were then translated into scientific names using the available literature and databases (Lundell, 1937; Standley and Steyermark, 1946; Schulze and Whitacre, 1999; Martínez and Galindo-Leal, 2002; Atran et al., 2004), while some plant specimens were compared with taxonomic types from the Paris Herbarium in France's National Museum of Natural History (MNHN). However, the local nomenclature of Naachtun plants contains many synonymies (one local name = different taxa) or polynomials (several local names = one taxon). To resolve this issue, we chose to apply taxonomic corrections, such as the following:

- Multiplication of nomen: *zakate* is used to designate both *Kyllinga pumila*, a Cyperaceae, and *Olyra latifolia*, a Poaceae. In these cases, the vernacular name, nomen, was used several times, to allow for better taxonomic and ecological representativeness.

- Construction of species complex: *Manilkara chicle*, *Pouteria glomerata*, *Pouteria reticulata*, *Sideroxylon tepicense*, trees belonging to the Sapotaceae family, are all named *zapote* or *zapotillo*. In such cases, we decided to group all these scientific names under the nomen *zapote*. Phytoliths do not allow for differentiation between woody dicotyledon species. We, therefore, chose to create species complexes for trees (62 nomens associated with woody dicotyledons). Phytoliths are, however, a good tool for characterizing monocotyledon families, such as Arecaceae, Cyperaceae, Commelinaceae, Musaceae, and Poaceae (Piperno, 2006; Honaine et al., 2009; Eichhorn et al., 2010; Novello et al., 2012; Chen and Smith, 2013). With some families, it is sometimes possible to determine the genus or species. Thus, for herbaceous plants, we multiplied the nomens to allow for better ecological monitoring using phytoliths (18 nomens). Finally, from the 157 initial occurrences, 75 nomens were assigned to a genus and five nomens to a family (See Table 3 in appendix). It should be noted that these sampling and identification methods were designed to be used primarily on ecological rather than taxonomic assemblages.

Plant associations were studied by quadrat using a statistical study of nomen occurrences. Each nomen class selected was classified for each of the quadrats based on the following criteria: Absent (0 occurrences), Present (1 to 8 occurrences) or Abundant (> 8 occurrences) (Table 3). These occurrence data (coded 0, 1 and 2 respectively) were studied using a hierarchical bottom-up classification coupled with a factor analysis of the correspondences. This statistical methodology aimed to verify the representativeness of the assemblages across the site and compare them with the literature (Lundell, 1937; Schulze and Whitacre, 1999; Martínez and Galindo-Leal, 2002).

3.2. Preparation and counting of phytolithes

The procedure for phytolith extraction was adapted from Piperno (2006). For approximately 20 g of soil: (1) Organic Matter was destroyed using hydrogen peroxide (H_2O_2), (2) clays were deflocculated using sodium hexametaphosphate (SHMP; 40 g/L), (3) sand and gravel were removed by sieving at 250 µm, (4) clays were eliminated by draining, and (5) amorphous siliceous matter

was concentrated and extracted by densimetric sorting using sodium polytungstate diluted to a density of 2.30–2.35.

The dried residue was mounted on microscope slides in immersion oil to allow rotation and 3-D analysis. Observations, identifications, and counts were performed under a microscope at magnifications between x450 and x630. As counting methods influence the ecological interpretation of phytolith assemblages, we followed recommendations in counting at least 200 diagnostic phytolith morphotypes for each sample (Stomberg, 2009; Zurro, 2017). In addition to these diagnostic phytoliths, we also counted non-diagnostic phytolith morphotypes, sponge spicules, and diatoms. The results are presented in a diagram of the relative abundances of diagnostic morphotypes. The diagram also includes the relative abundances of non-diagnostic shapes and bioindicators, calculated as the total sum of all particles counted.

3.3. Classification of phytolithes

Although phytolith assemblages in the forests of Petén have not yet been studied, other forests in intertropical zones have been the subject of studies, such as those from Amazonia (Piperno 1988; Dickau et al. 2013; Watling et al. 2016), Africa (Alexandre et al, 1997; Barboni et al. 1999; Runge 1999; Aleman et al., 2012), Indonesia (Chabot et al., 2018) and New Guinea (Boyd et al., 1998). Others researches conducted on current Central and South American plant phytoliths complete this first overview (Piperno and Pearsall, 1998; Iriarte, 2003; Iriarte et al., 2009; Watling and Iriarte, 2013). Our phytolith classification (Table 1) is based on these regional studies and other work (Iriarte, 2003; Eichhorn et al., 2010; Fenwick et al., 2011; Collura and Neumann, 2017; Neumann et al., 2017), as well as the nomenclature of the ICPN working group (Madella et al., 2005).

3.3.1. Sclereid shapes (Plate I, a-c)

The sclereids represent a particular group associated with the sclerenchyma of woody dicotyledons (Piperno, 2006) and for which the nomenclature is not well established. Many morphotypes have been described in the literature; the majority exceed 50 µm and can reach up to 200 µm. Some are elongated (Postek, 1981; Runge, 1999; Piperno, 2006; Garnier et al., 2013) or polyhedral with a smooth, faceted surface and relatively thick edges (Kealhofer and Piperno, 1998; Runge, 1999; Neumann, 2009; Garnier et al., 2013). Other morphotypes are larger, three-dimensional and irregular in shape, with a smooth surface (Runge, 1999; Stromberg, 2004; Garnier et al., 2013). It is also possible to find variants of this more regular morphotype in the form of large, smooth polyhedral with well-defined faces (Mercader et al., 2009; Garnier et al., 2013). Finally, smaller, undefined shapes, between 20 and 60 µm, may show protuberances or growths on their surface (Garnier et al., 2013; Collura and Neumann, 2017). All of these morphotypes, belonging to the large sclereid class, have been identified in the leaves, wood, and bark of many woody plants (Runge, 1999; Piperno, 2006; Collura and Neumann, 2017).

3.3.2. Globular shapes (Plate I, d-k)

Spherical to ellipsoid shapes can be differentiated from their ornamentation. Globular shapes with a smooth surface have been identified many times in the tissues of woody dicotyledons (Wilding and Drees, 1973; Piperno, 1988; Iriarte and Paz, 2009; Watling and Iriarte, 2013), as well as in some monocotyledons (Runge, 1999; Bremond et al., 2004). The globular decorated shapes (warty, rough, crenellated, aggregate, etc.; Plate I, f-g) described in the literature (Piperno, 1988; Alexandre et al., 1997; Kealhofer and Piperno, 1998; Barboni et al., 1999; Iriarte and Paz, 2009; Garnier et al., 2013) are produced in the fruits, leaves and wood of woody dicotyledonous. Sometimes the globular morphotypes are formed of aggregate particles, named globular compound (Garnier et al., 2013; Collura and Neumann, 2017), or angular particles, named globular nodular (Neumann et al., 2009; Collura and Neumann, 2017). In our study, all these shapes are classified under the "globular mixed" category.

We chose to create a separate category for globular faceted morphotypes (Plate I, d), as they are characteristic of the Cucurbitaceae family (Piperno et al., 2000; Piperno, 2006), one of the key crops of Maya societies.

The last globular morphotype is the globular echinate (Plate I, i-k). It is a spheroid shape covered with tips. This morphotype, widely observed in the literature, is generally associated with Arecaceae (Tomlinson, 1961; Piperno, 1988; Kealhofer and Piperno, 1998; Runge, 1999; Dickau et al., 2013; Watling et al., 2016). However, the production of this morphotype depends on the subfamily (Thomas, 2011).

3.3.3. Hat-shapes

This hat-shape morphotype (Plate I, l) is a semi-spherical shape crowned by one and several thorns. It is relatively small in size: less than 25 µm (Piperno, 1988, 2006; Kealhofer and Piperno, 1998; Dickau, 2013; Iriarte and Watling., 2013; Watling et al., 2016). It is generally associated with Arecaceae but is more representative of certain subfamilies, such as Arecoideae (Thomas, 2011).

3.3.4. Grass short-cell phytolith (GSCP) shapes (Plate I, m-aa)

The grass short-cell phytoliths (GSCPs) are divided into three main morphotypes: the lobate, saddle and rondel shapes. These three classes of phytoliths represent a great diversity of shapes and can be divided into numerous sub-variants (Mulholand, 1989; Piperno and Pearsall, 1998; Barboni and Bremond, 2009; Novello et al., 2012; Neumann et al., 2017). Barboni and Bremond (2009) suggest that the multiplication of sub-variants reduces the effects of taxonomic redundancy within the subfamilies of Poaceae. However, other researchers claim that the development of a complex classification system, with characters that are not objective and therefore difficult to reproduce from one author to another, has led to an increase in the various forms and thus to errors in the interpretation of assemblages (Rovner, 1971; Neumann et al., 2017). In our study, we chose to use

this last approach to GSCP classification to build our base (Barboni and Bremond, 2009; Neumann et al., 2017).

Lobate shapes are mainly produced by Panicoideae (Twiss, 1992; Piperno and Pearsall, 1998; Piperno, 2006). There are three main variants: bilobate (Plate I, m-p), cross (Plate I, q-s) and polylobate (Plate I, u-v) shapes. The classification proposed by Neumann et al. (2017) classifies bilobate and cross shapes according to particle size and shank length. This is particularly important in our study, as it has been shown that the size of crosses could be an indicator of domesticated Zea mays (Prat, 1948; Pearsall and Piperno, 1990; Iriarte, 2003). Polylobate shapes (Plate I, u-v) and other rare shapes of lobate (e.g. triangle cross, Plate I, t) are not subdivided into variants. Saddle-shaped GSCPs are produced by Chloridoideae (Barboni and Bremond, 2009; Garnier et al., 2013). Because Neumann et al. (2017) point out that the different shapes of saddles can't be assigned to taxonomic classification, we chose to view saddles (Plate I, w-x) as a single class of GSCP.

The rondel morphotypes (Plate I, y-aa) show relatively large morphological variation (Mulholand, 1989; Novello et al., 2012), but are not characteristic of a Poaceae subfamily (Barboni and Bremond, 2009; Neumann et al., 2017). Thus, in our classification, rondel shapes are classified into one morphotype, except for two particular shapes (Plate I, y-z). Pearsall et al. (2003) identified a rondel shape recognizable by a top with three spaced ridges (Plate I, aa) that is both corn and teosinte specific in the Maya zone. Given the importance of maize to Maya societies, we decided to keep apart this morphotype.

3.3.5. Papillae shapes (Plate I, ab-ag)

Papillae phytolith morphotypes are associated with Cyperaceae (Ollendorf et al., 1992; Runge, 1999; Thorn, 2004; Lu et al., 2006; Honaine et al., 2009; Neumann et al., 2009; Garnier et al., 2013; Novello et al., 2018). From our observations, most papillae morphotypes have a swelling that is angular or rounded, relatively large, and generally in the center of the shape. This lump

appeared hollow on all morphotypes observed. Studies have shown that, currently, it is not possible to discuss its taxonomic assignment more precisely (Ollendorf et al., 1992; Honaine et al., 2009). Nevertheless, each variant of papillae morphotype has been retained in our classification. The distinctive characteristics of these variants are the general shape of the plate, its texture, the ornamentation of the margins, and finally the size and structure of the luminous core.

3.3.6. Non-diagnostic shapes and other bioindicators (Plate II)

Some phytolith morphotypes are considered not diagnostic such as bulliform cells and elongate shapes. Bulliform cells are produced in the epidermis of plant leaves, from both monocots and dicots (Piperno, 2006). They are rather large morphotypes, generally > 20 µm, with various morphologies. In our study, we identified three bulliform shapes: cuneiform (Plate II, a-b), smooth parallelepiped (Plate II, c-d) and ornamented parallelepiped (Plate II, e-f). Although they do not have a taxonomic role, these shapes can nevertheless provide information on the ecological parameters of the deposition site, and the availability of water for certain plants in particular (Bremond et al., 2004). The second non-diagnostic phytolith family is that of the elongate morphotypes (Plate II, g-k). They are produced both in the tissues of herbaceous plants (Twiss et al., 1969; Lu and Liu, 2003) and dicotyledons (Piperno, 1988; Runge, 1999). Two subtypes can be discerned: elongate smooth shapes and elongate decorated shapes.

Finally, in our non-diagnostic counts, we included sponge spicules and diatoms (Plate II, l-s). These non-phytoliths siliceous forms are associated with water environments and can provide information about wetlands.

3.3.7. Use of phytolithic indices

The D/P index was developed to describe the density of tree cover (Alexandre et al., 1997). It is calculated as a ratio of globular shapes associated with dicotyledons to GSCPs (Alexandre et

al., 1997; Barboni et al., 1999; Bremond et al., 2004). Until now, this index has been little used in American tropical environments (Dickau et al., 2013). In this study, we tested its effectiveness in neotropical zones.

3.4. Statistical analysis

The statistical analysis in this study aims to attest our observations in the field, as well as the results from counting the phytolith assemblages. The statistical analysis of the quadrats, which had been grouped according to the main types of plant community, was carried out in two stages. The vegetation quadrat groupings were tested by a dissimilarity analysis using HAC (Hierarchical Agglomerative Clustering) clusters. It allows verifying whether quadrat groupings in ecosystems are represented by at least one similarity index, to identify poorly defined quadrats and ultimately to justify our groupings in the following factor analysis. The second step in the statistical analysis of modern vegetation environments is a component analysis. This method allowed to assign groups based on the data matrix and identify the main characteristics that contribute to this graphical morphology: namely, plant taxa. A component analysis was performed on the quadrat/phytolith data matrices. By using the plant groups identified by the HAC the scatter plot obtained by analyzing the phytoliths was compared with the analysis of the current plant communities, and at the same time, the coherence between modern plant communities and phytolith assemblages was tested.

4. Results

4.1 Botanical study: Plant communities at the Naachtun site

The study of plant communities along the four transects from the *bajos* at low altitudes to the hills identified six major types of plant communities (Fig. 2 and 3). These field observations were tested by the use of a correspondence analysis.

4.1.1. The *Sival* zone (Plate III, f)

Today, almost the entire Naachtun site is covered by forest. The only exception is the *Sival* zone, located in the northern *bajo,* which is characteristic of a wet savannah composed of *zakaton* (*Phragmites australis*) and *tul* (*Cyperus articulates*). The wet nature of the *Sival* is supported by the presence of *lechuga* (*Pistia stratiotes*). On the edge of the water area, an association of *yerba buena* (*Mentha x piperita*) and *zarza* (*Mimosa pigra*) was observed. Wild squash, *calabaza de raccoon* (*Cucurbita radicans*), was also observed at the edge of the *Sival* zone along transect T3. This association on the edge of a *Sival* zone had already been observed in Naachtun's northern *bajo* by Lundell in 1937 and was also reported by Martinez and Galindo-Leal in the Calakmul area in 2002 under the name *savana humeda*.

4.1.2. The *Tintal* zone (Plate III, e)

The *Sival* areas are bordered by a low forest dominated almost entirely by the *tinto* (*Haematoxylum campechianum*), a small knotty tree, cracked bark, with thorny branches and small leaves. These anatomical characteristics correspond to the usual adaptations of xerophytic vegetation in areas with high desiccation and strong sunlight. The name of this area, *Tintal,* can be explained by the predominance of this tree species. There is also a small *Tintal* zone in the southern *bajo* (quadrat S35, transect T4, Fig. 3). This type of environment has been recorded throughout northern Petén and appears characteristic of *bajo* areas bordering *aguadas (wetland)* (Lundell, 1937; Schulze and Whitacre, 1999; Martinez and Galindo-Leal, 2002).

4.1.3. The *Chechemal* zone (Plate III, d)

Further away from the *Sival* zone, the concentration of *tinto* decreases and is replaced by associations of shrubs belonging to the Anacardiaceae, Euphorbiaceae, Fabaceae and Myrtaceae families, such as *chechem negro* (*Metopium brownei*), *subin*, *katsin* and *jiesmo* (*Acacia sp*.), *cascarillo* (*Croton sp*) and *guayavillo* (*Eugenia* sp.). The *Chechemal* zones, being those furthest from the water areas, contain some palm species, such as *cambray* (*Chamaedorea seifrizii*) and *escobo* (*Cryosophila stauracantha*). The herbaceous stratum is poorly represented, with some sparse *zakate I* (*Olyra latifolia*), *zakate II* (*Kyllinga pumila*), *zakate III* (*Cyperus ochraceus*) and *zakate de huecht* (*Rhynchospora cephalotes*). Plant species are widely dispersed in *Chechemal* environments, and their relative proportions may vary depending on the geographical area studied. Lundell (1937) does not seem to consider this plant community to be a *bajo* environment, but rather an area of secondary regrowth. Martinez and Gallindo-Leal (2002) found the same association in the Calakmul region and named it *bajo mixto*. Tikal, Schulze and Whitacre (1999) considered these species associations to be a swamp forest environment distinct from the *Tintal* forest. We chose to name this environment *Chechemal* due to the presence of a particular tree, the *chechem negro* (*Metopium Brownei*).

4.1.4. The *Escobal* zone (Plate III, c)

The northern slopes of the *bajo* and the eastern slopes of the southern *bajo* are covered by dense forest, higher than the *bajo* forests, and dominated by palm trees of the *escobo* (*Cryosophila stauracantha*) variety. Those are secondary species habitually growing in the higher areas of the site as well as *Chechemal* zones. Herbaceous plants are rare: *zakate* (*Olyra latifolia*) was observed only rarely. These dense palm forests are interpreted as the transition forests in the literature and referred to *Escobal* by Lundell (1937). They are found on the non-flooded slopes of transects T1, T3, and T4, and on the margins of the *bajo* zone along T2 (Fig. 2 and Fig. 3).

4.1.5. The *Ramonal/Zapotal* zone (Plate III, a)

The main vegetation on the archaeological site and hilly areas is a high forest dominated by trees up to 40 meters high belonging to the Sapotaceae, Sapindaceae, Myrtacae, and Moraceae. The most representative trees of this forest are the *ramon* (*Brosimum alicastrum*) and the *chicozapote* (*Manilkara zapota*). It can explain why two types of high forests were identified by Lundell (1937) and Schulze and Whitacre (1999): the *Ramonal* and *Zapotal* high forests. The *Ramonal* areas are characterized by a large population of *ramon* and an undergrowth rich in populations of *xate* (*Chamaedorea sp*.) and *cordoncillo* (*Piper* sp.). The forests of *Zapotal* are rich in Sapotaceae species and have relatively low palm undergrowth. In 1938, Lundell proposed that the domination of these resource-producing trees over the site areas should be inherited from old maintained gardens. In this study, we consider these forest communities as a single forest named here *Ramonal/Zapotal* area. In these forest environments, herbaceous plants are rare: only *zakate* (*Olyra latifolia*) is occasionally found.

4.1.6. The *Carrizal* zone (Plate III, b)

Locally, we observed some open patches in the *Ramonal*/*Zapotal* zone (T1 and T4) characterized by dense herbaceous thickets, which we refer to as *Carrizal* zones. Observed by Lundell in Naachtun in 1937, they consist of juvenile bamboos called *carrizo* (*Rhipidocladum bartlettii*). Concentrations of grass are relatively rare at the Naachtun site, meaning that the *Carrizal* zone can be considered one of its typical plant associations. *Carrizal* areas do not appear to be particularly associated with topographical or edaphic conditions, or archaeological structures.

4.2. Statistical tests of plant communities

We first used hierarchical cluster analysis to assess the validity of grouping the environments into six ecosystems (Fig. 4). The HAC checks, in the form of a cluster, whether a

hierarchy index finds initial groupings. In our case, the Euclidean hierarchy index was the most consistent. Nonetheless, five samples (S01, S02, S16, S22, and S24) do not correspond to our initial classification. With this HAC, S22 was interpreted as *Escobal* vegetation, while S24 was interpreted by the analysis as *Chechemal* vegetation. The three other quadrats clearly contained transitional vegetation and are defined as such in our statistical analysis.

The first two axes of the component analysis (CA) of all quadrats explain 25.0% of the total variance (Fig. 5a). The contribution tables of Fig. 5 show the species that contributed most to the morphology of the scatter plot and that are considered as ecological indicators. Axis 1 (14.6% of the variance) distinguishes open habitat quadrats with Sival species, located at the positive end, from forest quadrats, located at the negative end. Axis 2 (10.4% of the variance) distinguishes plant communities according to the main altitude ranges. Samples and species typical of *bajo* forests are located at the positive end, while forest samples from the archaeological site, more upper, are grouped at the negative end. Two irregularities were identified within this first CA. Quadrat S24 is interpreted to be a relatively open zone in the *bajo*, whereas it is a forest zone disturbed by a compacted path at the edge of a Sival zone. This observation leads us to conclude that this sample is problematic. The second problem is that the scatter plot corresponding to the hill vegetation environments is too condensed to discriminate the quadrats. Thus, to refine our classification, we chose to perform a second CA on these samples (Fig. 5b).

For the second CA, the first three axes explain 35% of the variance. The CA conducted on the first two axes (Fig. 5b) shows that Axis 2, which explains 11.1%, is not decisive in the distribution of samples and species. Axis 1 (15.3% of the variance) distinguishes the quadrats associated with the *bajo* areas located at its negative end from the hill and site quadrats at its positive end. Axis 3 (9.4% of the variance; Fig. 5c) distinguishes the forest areas of hills with samples of the *Ramonal/Zapotal* zones at its negative end, and samples of *Carrizal* environments at its positive end

These conclusive statistical analyses demonstrate that our sampling and botanical survey method is statistically reliable, except for the identified plant transition zones. Thus, this classification of plant communities can be used to characterize modern phytolith assemblages.

4.3. Modern phytolith assemblages (Fig. 6 and Fig. 7)

The phytoliths counts from each quadrat have been summarized in Fig. 6 and Fig. 7. The distribution diagram (Fig. 6) shows the relative abundances of phytolith morphotypes by quadrat, grouped into plant communities. The first part of the diagram concerns the relative abundances of diagnostic morphotypes. They are expressed as a percentage of the total number of diagnostic morphotypes. The second part of the diagram concerns the abundance of non-diagnostic phytoliths and bioindicators. They are expressed as a percentage of the total number of counted particles. The diagram of the descriptive statistics for the morphotypes (Fig. 7) shows the amplitude of the distribution of morphotype classes across the six types of plant communities. This second diagram completes the relative abundances diagram. On these diagrams, quadrats that were not discriminated by the HAC (Fig. 4; S1, S2, and S16) were not included in the calculations in Fig. 7.

Sival: Six samples are assigned to this environment (S10, S11, S12, S25, S26, and S27). The phytolith assemblages are dominated by globular mixed, GSCP (especially saddle and rondel) and papillae morphotypes. On average, papillae morphotypes represent 35% of *Sival* assemblages, reaching up to 85% in S10. Globular mixed, saddle and rondel phytoliths represent on average 15% of *Sival* assemblages but could account for over 30% (Fig. 6). The D/P index accounts systematically less than 1. For bioindicators, *Sival* environments record the highest average proportion of sponge spicules (30%) and diatoms (6%) of all assemblages. Analysis of the relative abundance diagram points to differences between the assemblages in forest environments (*Ramonal, Carrizal, Escobal, Chechemal,* and *Tintal*) and wet/open environments (*Sival*; Fig. 6).

Tintal: Four samples are assigned to this environment (S9, S13, S28, and S35). The phytolith assemblages are dominated by globular mixed, GSCP (lobate) and papillae morphotypes.

On average, globular mixed morphotypes represent 37% of *Sival* assemblages, reaching up to 50% in S9 and S28 (Fig. 6 and Fig. 7). Lobate and papillae morphotypes each account for on average 21% of *Tintal* assemblages (Fig. 7). The D/P index oscillates between values close to 1. The proportions of bioindicators are close to those observed in the *Sival*, with an average of 28% for sponge spicules and 3% for diatoms.

Chechemal: Seven samples are assigned to this environment (S15, S24, S31, S32, S33, S34, and S36). The main feature is the high percentage of globular mixed shapes, accounting for on average 80% of assemblages but reaching up to 87% (S31 and S36; Fig. 6 and Fig. 7). Accordingly, the D/P index values are high (15–20). As regards bioindicators, diatoms are absent, while sponge spicules account for on average 8%.

Escobal: Eight samples are assigned to this environment (S9, S17, S18, S19, S20, S22, S23, and S37). Globular mixed (50%) and globular echinate (40%) phytoliths are predominant (Fig. 7). The D/P values are also very high, at 27 on average. The proportions of sponge spicules and diatoms in these assemblages are very low (less than 1% in average).

Carrizal: Four samples are assigned to this environment (S04, S07, S41, and S42). The phytolith assemblages are dominated by globular mixed morphotypes, exceeding 60%. The most conspicuous feature is the high percentage of rondel GSCPs, accounting for 26%, and the rondel crested morphotype, reaching values around 20% (Fig. 7). The non-diagnostic phytoliths, bulliform parallelepiped and elongate psilate morphotypes are particularly well represented in these samples (Fig. 6). The D/P values are low for a forest environment, recording 3 on average. Sponge spicules and diatoms are absent.

Ramonal/Zapotal: Eight samples are assigned to this environment (S3, S5, S6, S21, S38, S39, S40, and S43). Globular mixed and hat- shape morphotypes dominate these assemblages, representing 65% and 18% respectively. The D/P index is extremely high, with 38 on average. Sponge spicules and diatoms are absent.

4.4. Statistical tests of phytolith assemblages

538

539 The assembly groups defined based on the distribution diagram and ecosystems were tested
540 by a component analysis. The variables were the phytolith morphotypes and quadrat samples. The
541 contribution table of Fig. 8 indicates the morphotypes that contribute most to the morphology of the
542 scatter plot. Axis 1 and Axis 2 explain 52.7% of the variance (Fig. 8a). Axis 1, which explains
543 36.3% of the total variance, distinguishes between the openness and/or humidity of the
544 environments: the *Sival* and *Tintal* environments are located at the positive end and are mainly
545 influenced by sponge spicules, diatoms, and papillae morphotypes. GSCPs are also present at the
546 positive end. The negative side includes the samples taken from forest areas and morphotypes such
547 as globular mixed and globular echinate.

548 Axis 2 of our analysis explains 16.43% of the total variance and differentiates grassy
549 undergrowth forests from forest areas with trees only. The variables on the positive side of this axis
550 that contribute most to the morphology of the scatter plot are the rondel crested GSCP, bulliform
551 cells and elongate morphotypes. However, the samples from *Ramonal*, *Escobal* and *Chechemal*
552 forest areas form a group of samples that are difficult to analyze. This highlights the necessity of
553 isolating the *Carrizal* areas from the other forest areas on the site and in the *bajo*.

554 A second CA (Fig. 8b-c) was needed to distinguish the different Naachtun forest samples
555 (*Chechemal*, *Ramonal/Zapotal*, *Escobal*). The first three axes explained 73.5% of the total variance.
556 In the second graph (Fig. 8b), Axis 1 (29.2% of the variance) and Axis 2 (23.4% of the variance)
557 help to distinguish between the site's different forest ecosystems. The sponge spicules variable
558 contributes considerably to the morphology of the scatter plot for these two axes, and the
559 *Chechemal* samples are therefore located in the upper right corner of the graph and isolated from
560 the other samples. The second contributing variable for both axes is the globular echinate
561 morphotype, which is located on the negative part of Axis 1 and the positive part of Axis 2. This
562 morphotype allows to differentiate between the different *Escobal*-type forests (Fig. 8b). Axis 3 in
563 the second CA suggests that hat-shape morphotypes help to distinguish between the
564 *Ramonal*/*Zapotal* samples (Fig. 8c). Finally, the vegetation samples interpreted as "undefined

areas" by the HAC (S1, S2, and S16; Fig. 4), were not characterized by our component analysis either (Fig. 8).

5. Discussion

5.1. Definition and identification of Naachtun plant communities

The study and interpretation of phytolith assemblages show significant differences between plant formations. They point to the necessity of applying the general approach, as well as taking into account not only non-diagnostic phytoliths but also other bioindicators during the interpretation process.

The phytolith assemblages in *Sival* zones can be explained by their plant associations. Papillae morphotypes are produced by Cyperaceae, the family to which *tul* (*Cyperus articulatus*) belongs (Novello et al., 2012; Watling et al., 2013), while saddle and rondel morphotypes are produced by certain subfamilies of Poaceae, such as Arundinoideae, to which *zakaton* (*Phragmites australis*) belongs (Ollendorf et al., 1988; Piperno and Pearsall, 1998; Liu et al., 2013). The high proportions of diatoms could indicate the presence of perennial water.

The *Tintal* zones' assemblages were interpreted as assemblages of a transitional plant community between open and forest areas. The globular mixed phytoliths were most likely produced by *tinto* (*Haematoxylum campechianum*), which is the only woody dicotyledon in this plant community. The high proportions of papillae and bilobate morphotypes and other bioindicators can be explained by various processes. The *Sival* areas contained a much higher percentage of papillae morphotypes than in other studies (Barboni et al., 2007; Novello et al., 2012). The seasonal flooding of *Sival* areas may allow for the registration of Cyperaceae tissues and phytoliths, as well as diatoms and sponge spicules, in *Tintal* soils. Finally, the significant presence of bilobate morphotypes could be explained by the irregular presence of seasonal grassy undergrowth, consisting of Cyperaceae and Panicoideae, as was observed in 2017.

Chechemal forest assemblages can be partly explained by the rare occurrences of herbaceous species (Poaceae, Cyperaceae, etc.) or monocot trees, and by a predominance of the woody dicotyledons that produce globular mixed morphotypes. It is principally the presence of sponge spicules, due to seasonal flooding in these forest areas that permit these environments to be characterized.

The palm groves of the *Escobal* environments are characterized by a predominance of both globular echinate and globular mixed which morphotypes originating from the ligneous trees of the forest. The globular echinate morphotypes are produced by certain subfamilies of Arecaceae, such as Coryphoideae (Thomas, 2015), which *escobo* (*Cryosophila stauracantha*), the dominant species in this palm grove community, belongs to. The presence of sponge spicules indicates that these areas are subjected to a seasonal flood.

The *Ramonal*/*Zapotal* high forests are defined by a phytolith association composed of globular mixed and hat-shape morphotypes. Globular mixed morphotypes are produced by the woody dicotyledons of the forest, while hat-shape morphotypes may have originated from *xate* (*Chamaedorea sp.*), the dominant species in this plant community. Indeed, Thomas (2015) indicates that this morphotype is overrepresented in Arecoideae species, including the *Chamaedorea* genus. However, some samples (S6, S39, S40, and S43) contained lower proportions of hat-shape morphotypes (Fig. 6). This can be explained by the fact that the *Zapotal* plant association, described by Lundell (1937) and Schulze and Whitacre (1999), have undergrowth with lower *xate* content. This type of assemblage could, therefore, be confused with those in the upper areas of a *bajo* that do not contain sponge spicules (S01). Within the high forest vegetation, areas with bamboo thickets (*Carrizal*) were identified by an association of globular mixed, rondel crested, bulliform decorate and elongate smooth morphotypes. The fact that the undergrowth is dominated by *Rhipidocladum bartleddii* suggests that this bamboo species produce some of the morphotypes in this association. The discovery of similar rondel morphotypes in other bamboos (rondel three-pikes, Pearsall et al., 2003) may confirm this hypothesis.

To conclude, three levels of interpretation of the assemblages can be highlighted. (1) The first level concerns the differentiation between forest and open areas. High proportions of GSCPs and papillae shapes indicate open environments, while high proportions of globular mixed morphotypes, which may or may not be accompanied by palm tree morphotypes (globular echinate and hat-shape), are representative of forest environments. Forest zones with grassy undergrowth or "savannahs" are characterized by high proportions of globular mixed morphotypes and one or more morphotypes of GSCP or papillae, as in the case of the *Carrizal* and *Tintal* environments. (2) The second level of identification concerns the wet character of the vegetation. The presence of high proportions of papillae shapes (> 15%) in the assemblages indicates wet plant associations. As regards bioindicators, the presence of diatoms is associated with perennial water bodies, while sponge spicules suggest the presence of occasional or seasonal water bodies in the *bajo* zone. This is useful to identify the forest areas located in the *bajo*'s influence zone during the wet season. (3) The last level of interpretation of the diagrams concerns the identification of forest areas at the edges of hills, slopes, and *bajos*. At Naachtun, the proportion of phytoliths produced by the Arecaceae seems to be useful in distinguishing the palm transition forests and the *Ramonal* forest from the hills of the site.

5.2. Discussion of the use of indices

5.2.1. Identify the cover layer

The first studies conducted using the D/P index represented the tree cover as a ratio of globular decorated, produced by woody dicotyledons, to GSCPs and morphotypes associated by some authors with Poaceae (Alexandre et al., 1997, 1999; Bremond et al., 2004, 2008). Changes in the classification of phytoliths prompted the authors to adapt this formula to the morphotypes and environments studied (Stromberg, 2004; Bremond et al., 2004; Barboni et al., 2007; Neumann et al.,

2009; Garnier et al., 2013; Dickau et al., 2013). According to Alexandre et al. (1997), a D/P index > 1 is representative of open environments, while D/P values < 1 indicate forest areas.

Thus, for Naachtun plant environments, our results indicate that forest areas have high D/P values recording an average of 38 for *Ramonal/Zapotal* samples, 27 for *Escobal* samples and 16 for *Chechemal* samples. These values, higher than 1, are associated to dense vegetation areas, which is consistent with these forest environments. In the *Sival* samples without tree strata, the D/P index average was around 0.53, suggesting that the D/P index can be used to identify open environments. However, *Carrizal* areas, with grassy undergrowth, and *Tintal* areas, with seasonally grassy undergrowth, have D/P values higher than 1 but much lower than for forested areas. The average D/P index for *Carrizal* areas was 2.84, but varied between 1.1 and 6, while the index values for *Tintal* zones varied between 0.36 and 2.1 (Fig. 6, Fig. 9 and Fig. 10).

The D/P index does not seem suitable for identifying certain plant formations whose values overlap, such as those in the *Carrizal*, *Tintal* and *Sival* zones. This is particularly true of the *Tintal* and *Sival* environments, which contain similar phytolith assemblages dominating by Cyperaceae and GSCPs. To overcome this obstacle to interpretation, we decided to adjust the D/P formula to our study by including certain useful morphotypes (Cyperaceae, sclereid, globular echinate and hat-shape).

Fig. 9 shows the variation in the D/P values for each quadrat studied and compares them with the vegetation cover values for seven different D/P index formulae. The seven formulae correspond to a variation in the sum and type of morphotypes applied to the numerator, denominator, or both simultaneously (Table 2).

The first observation leads to the conclusion that including globular echinate and hat-shape morphotypes in the formula maximizes D/P values, especially for *Sival* zones where the D/P average was 0.9. Thus, the use of these morphotypes in the D/P formula does not seem justified. Including sclereid morphotypes in the index calculation does not have a significant effect on D/P values. This can be explained by the low proportions of this morphotype in the assemblages.

Including papillae morphotypes in the denominator of the index significantly reduces the index values for *Sival* (0.24 on average) and *Tintal* (0.98 on average) zones. If including papillae shapes minimize the values for *Tintal* zones, this highlights the opening of the *Sival* zones and therefore it seems necessary in our D/P index calculations. However, the simultaneous addition of sclereid morphotypes to the numerator and papillae morphotypes to the denominator increases the D/P values for *Tintal* zones (1.11 on average) while maintaining the best numerical representation of the *Sival* zones (0.29 on average). Thus, for the purposes of our study, and for geographical areas where papillae morphotypes make up a significant percentage of phytolith assemblages, we recommend to adjust the D/P index using the following formula:

Globular mixed + Sclereid / GSCP + Papillae

5.2.2. Identify the mixed zones

Even after adapting the D/P index to suit the particularities of our plant zones, it still does not seem possible to use the D/P index to identify mixed zones with grassy and woody layers. Indeed, our study shows that the D/P index for *Carrizal* and *Tintal* zones sometimes have the same values for *Sival* zone. It seems, therefore, necessary to develop a new index that allows these mixed zones, misinterpreted by the D/P index, to be clearly identified.

In this study, we propose a new index that defines a mixed zone characterized by a combination of woody trees and herbaceous plants as an addition D+P. This D+P assemblage must be matched with a tree D assembly and a grassy P assembly. We propose the following formula:

$$[((D+P)/P + (D+P)/D)/(D+P)]x10$$

which can be reduced to the form

[(D+P)/(D*P)]x10

The calculation of this formula implies that the predominance of any one part of the assembly (D or P) over the other parts will tend to minimize the denominator and thus produce high values indicating strictly forest or strictly savannah areas. Whereas a mixed assembly (D = P) will produce D/P index values of around 1, but this new index will allow the presence of both a herbaceous zone and tree stratum to be confirmed. Indeed, in such a case, the average values of D and P will increase the denominator, which will cause the index values to fall to a minimum value.

This new index, named LU (limits/undergrowth) index, was developed for our samples and has good potential for ecological recovery in our environmental contexts (Fig. 10). The lowest values were obtained for environments containing both a herbaceous stratum and tree cover, such as the *Carrizal* and *Tintal* environments. These LU values put into perspective the average D/P index values of these environments and confirm their mixed nature. The *Sival* zones generated different LU index values depending on the sampling zone. The values for quadrats S12, S25 and S27 were low and comparable to those of the *Carrizal* zones, which could be explained by the fact that the edges of the *Tintal* and *Ramonal* zones are located nearby. Conversely, the LU index values for the samples from the center of the *Sival* zone (S10, S11, and S26) were higher due to the distance from the wooded areas. The new index values calculated for the *Escobal* and *Ramonal* environments were relatively high and would indicate a sparse herbaceous stratum. This is in agreement with the high D/P index values. Finally, the *Chechemal* environment quadrats had relatively low values compared to other forest areas. Some of the low values from the new index (for quadrats S33 and S34) could correspond to forest areas where the herbaceous stratum is only seasonally present, as observed in other *bajo* areas at Naachtun. Based on the quadrats and vegetation parameters (tree cover, herbaceous undergrowth), we can define 0.25 as the maximum LU index value identifying mixed and transitional vegetation areas.

725 5.3. Development of a paleoenvironmental tool for Maya archaeology

726

727 One main objective of this study was to test the potential of phytolith assemblages in Petén
728 for characterizing past landscapes and past ecosystems. The main hurdles to the development of a
729 bioindicator tool are the different post-deposition taphonomic processes that can modify
730 thanatocoenosis and thus the interpretation of assemblages (Madella and Lancelotti, 2012). These
731 disturbance factors include the differential diagenetic recording of morphotypes (Piperno, 1988;
732 Alexandre et al., 1997), the vertical translocation of assemblages (Runge, 1999; Fishkis et al., 2010)
733 and lateral transport (Fredlund and Tieszen, 1994; Osterrieth et al., 2009; Madella and Lanceloti,
734 2012; Watling et al., 2016). Finally, factors making interpretation more difficult may also occur
735 during the production and deposition of phytoliths, depending on the composition of plant
736 communities and sediment types.

737 Initially, the analysis of fossil samples, and their palaeoenvironmental interpretation must be
738 carried out with the awareness that “time averaging” in Holocene sediment can easily represent
739 from several years to tens or hundreds of years (Fredlund and Tieszen, 1994; Albert et al., 2006).
740 For phytoliths records in fossil samples, it is difficult to know the period of the deposit. Thus, a
741 phytolith record contains a mixture of consecutive plant associations at a location over an unknown
742 number of years. However, this problem also exists for modern samples. The first centimeters of the
743 A horizon sampled are not representative of the current vegetation, but rather of the vegetation from
744 a recent period which is not precisely known and could cover several months to a few decades. The
745 part of transect T3 from the *Sival* zone to the southeast of the northern *bajo* (S24 to S27) is a good
746 example. The vegetation within the *Sival* zone is organized into specific vegetation rings linked to
747 the expansion of perennial water in spring: first the *tul*/*zakaton* association, then a halo of *tul* only,
748 then a *tul*/*yerba buena*/*zarza* association. As observed during field missions, every spring, water
749 availability is different, and this affects the plant composition of quadrats S24 to S28. It can link
750 with the spatial mobility of the *Sival* zone’s plant rings depending on water precipitation. Because it
751 is a continuous phenomenon continues, 2017 samplings in the eastern *Sival* zone may correspond to

752 an average of phytolith records from the vegetation at different seasons. Thus, in *Sival* assemblages,
753 the high proportions of papillae morphotypes represent the rings of *tul* (Cyperaceae), while high
754 proportions of saddle shapes represent the rings of *zakaton* (Arundinoideae), and globular mixed
755 and sclereid morphotypes indicate the rings of *zarza* (Fabaceae).
756 Phytolith assemblages can be affected by lateral transport effects, caused by wind, water,
757 gravity or bioturbation (Fredlund and Tieszen, 1994; Alexandre et al., 1997; Barboni et al., 1999;
758 Piperno, 2006). The systematic approach of ecological transect sampling allows to test the
759 estimation of morphotype transport from one quadrat to another one.Alexandre et al. (1997) point
760 out that high tropical forests' canopies limit wind transport. However, transport by water should be
761 accounted for interpreting assemblages. At Naachtun, phytolith transport by water may be
762 facilitated by the substantial drainage system from the high areas to the *bajo*, as well as the flooding
763 period of the *bajo* during the wet season. Our results show that phytolith assemblages are not
764 affected by transport and are most representative of the local vegetation. The vegetation of the
765 seasonally flooded lowlands (*Sival*, *Tintal*) is dominated by papillae polygonal and diatoms, while
766 globular mixed morphotypes are relatively few and mainly restricted to upper woody dicot areas.
767 The same observation can be made for the slope area samples. The drainage of high zones does not
768 result in the mixing of phytolith associations. For example, phytolith assemblages in the transition
769 area from S7 to S8 on transect T1 are not subject to contamination from rondel crested
770 morphotypes. Moreover, looking at the sloped area running along transect T3 (S22–S26), the upper
771 samples, which are rich in globular mixed morphotypes, have little influence on the D/P index value
772 for the *bajo* samples. Thus, for the current Naachtun site, phytolith transport plays a minor role in
773 the alteration of phytolith assemblages.
774 Transport does not affect the identification of plant landscapes. However, the transport of
775 phytoliths may play a role in the taxonomic representativeness of the quadrats studied. In all the
776 plant communities studied, palm phytoliths were observed in an average of around 5–10% of the
777 phytolith associations. In environments such as *Tintal* or *Sival* zones where Arecaceae are absent,
778 these high proportions of palm phytoliths raise questions over their transport. The high numbers of

phytoliths produced by the Arecaceae and their greater resistance to erosion (Chabot et al., 2018) could mean that they have a ubiquitous record. We surmise that comparable proportions (5–10%) of Arecaceae phytoliths in fossil samples can be interpreted as the result of contamination caused by transport, rather than as an identifying ecological signal.

6. Conclusion and Future Researches

This work has allowed for the development of a tool to study paleoenvironments in the Maya zone. Phytoliths are particularly useful in tropical forest areas where other types of fossil conservation can be lacking. The analysis of modern soil samples from Naachtun has shown the potential of phytolith assemblages as bioindicators of plant landscapes in the Maya zone. A robust interpretation of phytolith assemblages has been enabled both by sampling the modern soil and studying the modern plant communities' distribution. We used a general approach to interpret phytolith assemblages diagrams and multivariate statistical analyses, as well as an index approach. These results testify of the possibility to distinguish wet and open Sival areas from *bajo*, *Tintal* and *Chechemal* forest areas. The use of both phytoliths assemblages and phytolith indices seems to be particularly appropriate to differentiate opened, closed, and transitional plant environments. The consistency of the results between modern plant communities and phytolith assemblages demonstrates the validity of our methodology.

However, the environments of this study are only part of Petén environments. "Natural" and "anthropic" environments were certainly much more diversified in Maya times, and are still today. Thus, the realization of a current reference collection of phytoliths in anthropized areas is necessary to define more precisely the interpretation of the fossil phytolith assemblages from the occupation period of the Naachtun site. Some other environments, such as the savannahs of central Petén (Lundell, 1937) or the drier forests of northern Yucatán could have reached the Naachtun region during drier climatic periods. More humid environments of the lake or lagoon variety (Yaxha, Dos Lagunas, etc.) could also have been present during wet phases. Modern soil sampling of these

environments also seems necessary to construct a complete and current phytolith reference system for Maya environments on the Petén level.

Finally, the characterization of plant communities could be improved in taxonomic terms. As we have seen, the Naachtun ecosystems are mostly dominated by woody dicotyledons. A general study on the sclereids in such closed environments is needed to refine the taxonomic precision. More precise taxonomy could also be achieved by combining phytolith data with the data on other local bioindicators which are sensitive to variations in climatic parameters and ecological plant niches.

Acknowledgements

This research is supported by the Projet Naachtun 2010-2018 (Dir. Ph. Nondédéo), the Project HydroAgro (coord. E. Lemonnier et C. Castanet), The Project PAYAMA (coord. A. Garnier and E. Lemonnier), the LabEx DynamiTe (ComUE heSam), the Ministère des Affaires Etrangères (France), the Pacunam foundation, the Perenco company (Guatemala), the CNRS (France) and the Université de Paris 1 Panthéon Sorbonne. This research benefits from the institutional support of the Centro de Estudios Mexicanos y Centroamericanos (Guatemala).

References

Abramiuk, M.A., Dunham, P.S., Scott Cummings, L., Yost, C., Pesek, T.J., 2011. Linking Past and Present: A preliminary paleoethnobotanical study of Maya nutritional and medicinal plant use and sustainable cultivation in the Southern Maya Mountains, Belize. Ethnobot. Res. App. 9, 257. https://doi.org/10.17348/era.9.0.257-273

Abrams, E.M., Rue, D.J., 1988. The causes and consequences of deforestation among the prehistoric Maya. Hum Ecol 16, 377–395. https://doi.org/10.1007/BF00891649

Albert, R.M., Bamford, M.K., Cabanes, D., 2006. Taphonomy of phytoliths and macroplants in different soils from Olduvai Gorge (Tanzania) and the application to Plio-Pleistocene palaeoanthropological samples. Quaternary International 148, 78–94. https://doi.org/10.1016/j.quaint.2005.11.026

Aleman, J., Leys, B., Apema, R., Bentaleb, I., Dubois, M.A., Lamba, B., Lebamba, J., Martin, C., Ngomanda, A., Truc, L., Yangakola, J.-M., Favier, C., Bremond, L., 2012. Reconstructing savanna tree cover from pollen, phytoliths and stable carbon isotopes. J. Veg. Sci. 23, 187–197. https://doi.org/10.1111/j.1654-1103.2011.01335.x

Alexandre, A., Meunier, J.-D., Lézine, A.-M., Vincens, A., Schwartz, D., 1997. Phytoliths: indicators of grassland dynamics during the late Holocene in intertropical Africa. Palaeogeography, Palaeoclimatology, Palaeoecology 136, 213–229. https://doi.org/10.1016/S0031-0182(97)00089-8

Alexandre, A., Meunier, J.-D., Mariotti, A., Soubies, F., 1999. Late Holocene Phytolith and Carbon-Isotope Record from a Latosol at Salitre, South-Central Brazil. Quat. res. 51, 187–194. https://doi.org/10.1006/qres.1998.2027

Atran, S., Lois, X., Ucan Ek, E., 2004. Plants of the Petén Itza' Maya: Plantas de los maya itza' del Petén, Memoirs. Museum of Anthropology, University of Michigan, Ann Arbor.

Barboni, D., Bremond, L., 2009. Phytoliths of East African grasses: An assessment of their environmental and taxonomic significance based on floristic data. Review of Palaeobotany and Palynology 158, 29–41. https://doi.org/10.1016/j.revpalbo.2009.07.002

Barboni, D., Bonnefille, R., Alexandre, A., Meunier, J.D., 1999. Phytoliths as paleoenvironmental indicators, West Side Middle Awash Valley, Ethiopia. Palaeogeography, Palaeoclimatology, Palaeoecology 152, 87–100. https://doi.org/10.1016/S0031-0182(99)00045-0

Barboni, D., Bremond, L., Bonnefille, R., 2007. Comparative study of modern phytolith assemblages from inter-tropical Africa. Palaeogeography, Palaeoclimatology, Palaeoecology 246, 454–470. https://doi.org/10.1016/j.palaeo.2006.10.012

Beach, T., Luzzadder-Beach, S., Dunning, N., Cook, D., 2008. Human and natural impacts on fluvial and karst depressions of the Maya Lowlands. Geomorphology 101, 308–331. https://doi.org/10.1016/j.geomorph.2008.05.019

Beach, T., Luzzadder-Beach, S., Dunning, N., Jones, J., Lohse, J., Guderjan, T., Bozarth, S., Millspaugh, S., Bhattacharya, T., 2009. A review of human and natural changes in Maya Lowland wetlands over the Holocene. Quaternary Science Reviews 28, 1710–1724. https://doi.org/10.1016/j.quascirev.2009.02.004

Boyd, W.E., Lentfer, C.J., Torrence, R., 1998. Phytolith analysis for a wet tropics environment: Methodological issues and implications for the archaeology of Garua island, West New Britain, Papua New Guinea. Palynology 22, 213–228. https://doi.org/10.1080/01916122.1998.9989510

Bozarth, S.R., Guderjan, T.H., 2004. Biosilicate analysis of residue in Maya dedicatory cache vessels from Blue Creek, Belize. Journal of Archaeological Science 31, 205–215. https://doi.org/10.1016/j.jas.2003.08.002

Bremond, L., Alexandre, A., Véla, E., Guiot, J., 2004. Advantages and disadvantages of phytolith analysis for the reconstruction of Mediterranean vegetation: an assessment based on modern

phytolith, pollen and botanical data (Luberon, France). Review of Palaeobotany and Palynology 129, 213–228. https://doi.org/10.1016/j.revpalbo.2004.02.002

Bremond, L., Alexandre, A., Wooller, M.J., Hély, C., Williamson, D., Schäfer, P.A., Majule, A., Guiot, J., 2008. Phytolith indices as proxies of grass subfamilies on East African tropical mountains. Global and Planetary Change 61, 209–224. https://doi.org/10.1016/j.gloplacha.2007.08.016

Brenner, M., Hodell, D.A., Rosenmeier, M.F., Curtis, J.H., Binford, M.W., Abbott, M.B., 2001. Chapter 6 - Abrupt Climate Change and Pre-Columbian Cultural Collapse, in: Markgraf, V. (Ed.), Interhemispheric Climate Linkages. Academic Press, San Diego, pp. 87–103. https://doi.org/10.1016/B978-012472670-3/50009-4

Canuto, M.A., Estrada-Belli, F., Garrison, T.G., Houston, S.D., Acuña, M.J., Kováč, M., Marken, D., Nondédéo, P., Auld-Thomas, L., Castanet, C., Chatelain, D., Chiriboga, C.R., Drápela, T., Lieskovský, T., Tokovinine, A., Velasquez, A., Fernández-Díaz, J.C., Shrestha, R., 2018. Ancient lowland Maya complexity as revealed by airborne laser scanning of northern Guatemala. Science 361, eaau0137. https://doi.org/10.1126/science.aau0137

Carozza, J.-M., Galop, D., Metailie, J.-P., Vanniere, B., Bossuet, G., Monna, F., Lopez-Saez, J.A., Arnauld, M.-C., Breuil, V., Forne, M., Lemonnier, E., 2007. Landuse and soil degradation in the southern Maya lowlands, from Pre-Classic to Post-Classic times: The case of La Joyanca (Petén, Guatemala). Geodinamica Acta 20, 195–207. https://doi.org/10.3166/ga.20.195-207

Carrillo-Bastos, A., Islebe, G.A., Torrescano-Valle, N., 2012. Geospatial analysis of pollen records from the Yucatán peninsula, Mexico. Veget Hist Archaeobot 21, 429–437. https://doi.org/10.1007/s00334-012-0355-1

Castanet, C., Purdue, L., Lemonnier, E., Nondédéo, P., 2016. Dynamiques croisées des milieux et des sociétés dans les basses terres tropicales mayas : hydrosystème et agrosystème à Naachtun (Guatemala). Les nouvelles de l'archéologie 32–37. https://doi.org/10.4000/nda.3275

Chabot, Y., Garnier, A., Geria, I.M., 2018. Phytolith analysis from the archaeological site of Kota Cina (North Sumatra, Indonesia). Journal of Archaeological Science: Reports 20, 483–501. https://doi.org/10.1016/j.jasrep.2018.04.033

Chen, S.T., Smith, S.Y., 2013. Phytolith variability in Zingiberales: A tool for the reconstruction of past tropical vegetation. Palaeogeography, Palaeoclimatology, Palaeoecology 370, 1–12. https://doi.org/10.1016/j.palaeo.2012.10.026

Collura, L.V., Neumann, K., 2017. Wood and bark phytoliths of West African woody plants. Quaternary International, 9th International Meeting of Phytolith Research (IMPR) 434, 142–159. https://doi.org/10.1016/j.quaint.2015.12.070

Diamond, J.M., 2005. Collapse: how societies choose to fail or succeed. Viking, New York.

Dickau, R., Whitney, B.S., Iriarte, J., Mayle, F.E., Soto, J.D., Metcalfe, P., Street-Perrott, F.A., Loader, N.J., Ficken, K.J., Killeen, T.J., 2013. Differentiation of neotropical ecosystems by modern soil phytolith assemblages and its implications for palaeoenvironmental and archaeological reconstructions. Review of Palaeobotany and Palynology 193, 15–37. https://doi.org/10.1016/j.revpalbo.2013.01.004

Dunning, N.P., Luzzadder-Beach, S., Beach, T., Jones, J.G., Scarborough, V., Culbert, T.P., 2002. Arising from the Bajos: The Evolution of a Neotropical Landscape and the Rise of Maya

Civilization. Annals of the Association of American Geographers 92, 267–283. https://doi.org/10.1111/1467-8306.00290

Dussol, L., Elliott, M., Michelet, D., Nondédéo, P., 2017. Ancient Maya sylviculture of breadnut (Brosimum alicastrum Sw.) and sapodilla (Manilkara zapota (L.) P. Royen) at Naachtun (Guatemala): A reconstruction based on charcoal analysis. Quaternary International, Anthracology: Local to Global Significance of Charcoal Science - Part I 457, 29–42. https://doi.org/10.1016/j.quaint.2016.10.014

Ehrlich Paul R., Ehrlich Anne H., 2013. Can a collapse of global civilization be avoided? Proceedings of the Royal Society B: Biological Sciences 280, 20122845. https://doi.org/10.1098/rspb.2012.2845

Eichhorn, B., Neumann, K., Garnier, A., 2010. Seed phytoliths in West African Commelinaceae and their potential for palaeoecological studies. Palaeogeography, Palaeoclimatology, Palaeoecology 298, 300–310. https://doi.org/10.1016/j.palaeo.2010.10.004

Fedick, S.L., 2010. The Maya Forest: Destroyed or cultivated by the ancient Maya? PNAS 107, 953–954. https://doi.org/10.1073/pnas.0913578107

Fenwick, R.S.H., Lentfer, C.J., Weisler, M.I., 2011. Palm reading: a pilot study to discriminate phytoliths of four Arecaceae (Palmae) taxa. Journal of Archaeological Science, Satellite remote sensing in archaeology: past, present and future perspectives 38, 2190–2199. https://doi.org/10.1016/j.jas.2011.03.016

966 Fishkis, O., Ingwersen, J., Lamers, M., Denysenko, D., Streck, T., 2010. Phytolith transport in soil:
967 A field study using fluorescent labelling. Geoderma 157, 27–36.
968 https://doi.org/10.1016/j.geoderma.2010.03.012
969
970 Fredlund, G.G., Tieszen, L.T., 1994. Modern Phytolith Assemblages from the North American
971 Great Plains. Journal of Biogeography 21, 321–335. https://doi.org/10.2307/2845533
972
973 Garnier, A., Neumann, K., Eichhorn, B., Lespez, L., 2013. Phytolith taphonomy in the middle- to
974 late-Holocene fluvial sediments of Ounjougou (Mali, West Africa). The Holocene 23, 416–431.
975 https://doi.org/10.1177/0959683612463102
976
977 Hansen, R.D., Bozarth, S., Jacob, J., Wahl, D., Schreiner, T., 2002. Climatic and environmental
978 variability in the rise of Maya civilization: A preliminary perspective from northern Peten. Ancient
979 Mesoamerica 13, 273–295. https://doi.org/10.1017/S0956536102132093
980
981 Hastenrath, S., 1976. Variations in Low-Latitude Circulation and Extreme Climatic Events in the
982 Tropical Americas. J. Atmos. Sci. 33, 202–215. https://doi.org/10.1175/1520-
983 0469(1976)033<0202:VILLCA>2.0.CO;2
984
985 Hastenrath, S., 1984. Interannual Variability and Annual Cycle: Mechanisms of Circulation and
986 Climate in the Tropical Atlantic Sector. Mon. Wea. Rev. 112, 1097–1107.
987 https://doi.org/10.1175/1520-0493(1984)112<1097:IVAACM>2.0.CO;2
988
989
990 Hodell, D.A., Brenner, M., Curtis, J.H., Medina-González, R., Can, E.I.-C., Albornaz-Pat, A.,
991 Guilderson, T.P., 2005. Climate change on the Yucatan Peninsula during the Little Ice Age.
992 Quaternary Research 63, 109–121. https://doi.org/10.1016/j.yqres.2004.11.004

Honaine, M.F., Zucol, A.F., Osterrieth, M.L., 2009. Phytolith analysis of Cyperaceae from the Pampean region, Argentina. Aust. J. Bot. 57, 512–523. https://doi.org/10.1071/BT09041

Iriarte, J., 2003. Assessing the feasibility of identifying maize through the analysis of cross-shaped size and three-dimensional morphology of phytoliths in the grasslands of southeastern South America. Journal of Archaeological Science 30, 1085–1094. https://doi.org/10.1016/S0305-4403(02)00164-4

Iriarte, J., Paz, E.A., 2009. Phytolith analysis of selected native plants and modern soils from southeastern Uruguay and its implications for paleoenvironmental and archeological reconstruction. Quaternary International, Perspectives on Phytolith Research: 6th International Meeting on Phytolith Research 193, 99–123. https://doi.org/10.1016/j.quaint.2007.10.008

Islebe, G.A., Hooghiemstra, H., Brenner, M., Curtis, J.H., Hodell, D.A., 1996. A Holocene vegetation history from lowland Guatemala. The Holocene 6, 265–271. https://doi.org/10.1177/095968369600600302

Kealhofer, L., Piperno, D.R., 1998. Opal Phytoliths in Southeast Asian Flora. Smithsonian Contributions to Botany 1–39. https://doi.org/10.5479/si.0081024X.88

Lentz, D.L., Hockaday, B., 2009. Tikal timbers and temples: ancient Maya agroforestry and the end of time. Journal of Archaeological Science 36, 1342–1353. https://doi.org/10.1016/j.jas.2009.01.020

Lentz, D.L., Magee, K., Weaver, E., Jones, J.G., Tankersley, K.B., Hood, A., Islebe, G., Ramos Hernandez, C.E., Dunning, N.P., 2015. Agroforestry and Agricultural Practices of the Ancient

Maya at Tikal, in: Lentz, D.L., Dunning, N.P., Scarborough, V.L. (Eds.), Tikal. Cambridge University Press, Cambridge, pp. 152–185. https://doi.org/10.1017/CBO9781139227209.009

Leyden, B.W., 2002. Pollen evidence for climatic variability and cultural disturbance in the maya lowlands. Ancient Mesoamerica 13, 85–101. https://doi.org/10.1017/S0956536102131099

Liu, L., Jie, D., Liu, H., Li, N., Guo, J., 2013. Response of phytoliths in Phragmites communis to humidity in NE China. Quaternary International 304, 193–199. https://doi.org/10.1016/j.quaint.2013.03.020

Lu, H., Liu, K., 2003. Phytoliths of common grasses in the coastal environments of southeastern USA. Estuarine, Coastal and Shelf Science 58, 587–600. https://doi.org/10.1016/S0272-7714(03)00137-9

Lu, H.-Y., Wu, N.-Q., Yang, X.-D., Jiang, H., Liu, K., Liu, T.-S., 2006. Phytoliths as quantitative indicators for the reconstruction of past environmental conditions in China I: phytolith-based transfer functions. Quaternary Science Reviews 25, 945–959. https://doi.org/10.1016/j.quascirev.2005.07.014

Lundell, C.L., 1932. Exploring Nohoxna: A Lost City of the First Maya Empire. Southwest Review 17, 395–406.

Lundell, C.L., 1937. The Vegetation of Peten. Carnegie Institution, Washington, D.C.

Lundell, C.L., 1938. Plants probably utilized by the old empire Maya of Petén and adjacent lowlands. Papers of the Michigan Academy of Science, Arts, and Letters 24, 37–56. https://babel.hathitrust.org/cgi/pt?id=mdp.39015071693415&view=1up&seq=63

Madella, M., Alexandre, A., Ball, T., 2005. International Code for Phytolith Nomenclature 1.0. Ann Bot 96, 253–260. https://doi.org/10.1093/aob/mci172

Madella, M., Lancelotti, C., 2012. Taphonomy and phytoliths: A user manual. Quaternary International 275, 76–83. https://doi.org/10.1016/j.quaint.2011.09.008

Martínez, E., Galindo-Leal, C., 2017. La vegetación de Calakmul, Campeche, México: clasificación, descripción y distribución. Bot. Sci. 7. https://doi.org/10.17129/botsci.1660

McNeil, C.L., 2012. Deforestation, agroforestry, and sustainable land management practices among the Classic period Maya. Quaternary International 249, 19–30. https://doi.org/10.1016/j.quaint.2011.06.055

Meadows, D.H., Randers, J., Meadows, D.L., 2004. The limits to growth: the 30-year update. Chelsea Green Publishing Company, White River Junction, Vt.

Mercader, J., Bennett, T., Esselmont, C., Simpson, S., Walde, D., 2009. Phytoliths in woody plants from the Miombo woodlands of Mozambique. Annals of Botany 104, 91–113. https://doi.org/10.1093/aob/mcp097

Mulholland, S.C., 1989. Phytolith shape frequencies in North Dakota grasses: a comparison to general patterns. Journal of Archaeological Science 16, 489–511. https://doi.org/10.1016/0305-4403(89)90070-8

Neumann, K., Fahmy, A., Lespez, L., Ballouche, A., Huysecom, E., 2009. The Early Holocene palaeoenvironment of Ounjougou (Mali): Phytoliths in a multiproxy context. Palaeogeography, Palaeoclimatology, Palaeoecology 276, 87–106. https://doi.org/10.1016/j.palaeo.2009.03.001

Neumann, K., Fahmy, A.G., Müller-Scheeßel, N., Schmidt, M., 2017. Taxonomic, ecological and palaeoecological significance of leaf phytoliths in West African grasses. Quaternary International, 9th International Meeting of Phytolith Research (IMPR) 434, 15–32. https://doi.org/10.1016/j.quaint.2015.11.039

Nondédéo, P., Morales-Aguilar, C., Patiño, A., Forné M., Andrieu C., Sion, J., Michelet, D., Arnauld, M-C., Gillot, C., de León, M., Cotom, J., Lemonnier, E., Pereira, G., and Barrientos, I., 2012. Prosperidad económica en Naachtun: resultados de las dos primeras temporadas de investigación, in: Arroyo, B., Paiz Aragon, L., and Mejia, H. (Eds.), XXV Simposio de Investigaciones Arqueológicas en Guatemala. Museo Nacional de Arqueología y Etnología, Asociación Tikal, Guatemala, pp. 227-235. http://www.asociaciontikal.com/wp-content/uploads/2017/03/019_Nondedeo_2.pdf

Nondédéo, P., Patiño, A., Sion, J., Michelet, D., and Morales-Aguilar, C., 2013. Crisis multiples en Naachtún: aprovechadas, superadas e irreversibles. Millenary Maya Societies: Past Crises and Resilience, 122-147. http://mesoweb.org/publications/MMS/9_Nondedeo_etal.pdf

Novello, A., Barboni, D., Berti-Equille, L., Mazur, J.-C., Poilecot, P., Vignaud, P., 2012. Phytolith signal of aquatic plants and soils in Chad, Central Africa. Review of Palaeobotany and Palynology 178, 43–58. https://doi.org/10.1016/j.revpalbo.2012.03.010

Novello, A., Bamford, M.K., van Wijk, Y., Wurz, S., 2018. Phytoliths in modern plants and soils from Klasies River, Cape Region (South Africa). Quaternary International 464, 440–459. https://doi.org/10.1016/j.quaint.2017.10.009

Ollendorf, A.L., 1992. Toward a Classification Scheme of Sedge (Cyperaceae) Phytoliths, in: Rapp, G., Mulholland, S.C. (Eds.), Phytolith Systematics: Emerging Issues, Advances in Archaeological and Museum Science. Springer US, Boston, MA, pp. 91–111. https://doi.org/10.1007/978-1-4899-1155-1_5

Ollendorf, A.L., Mulholland, S.C., Rapp, G., 1988. Phytolith Analysis as a Means of Plant Identification: Arundo donax and Phragmites communis. Ann Bot 61, 209–214. https://doi.org/10.1093/oxfordjournals.aob.a087544

Osterrieth, M., Madella, M., Zurro, D., Fernanda Alvarez, M., 2009. Taphonomical aspects of silica phytoliths in the loess sediments of the Argentinean Pampas. Quaternary International 193, 70–79. https://doi.org/10.1016/j.quaint.2007.09.002

Pearsall, D.M., Piperno, D.R., 1990. Antiquity of Maize Cultivation in Ecuador: Summary and Reevaluation of the Evidence. American Antiquity 55, 324–337. https://doi.org/10.2307/281650

Pearsall, D.M., Chandler-Ezell, K., Chandler-Ezell, A., 2003. Identifying maize in neotropical sediments and soilsusing cob phytoliths. Journal of Archaeological Science 30, 611–627. https://doi.org/10.1016/S0305-4403(02)00237-6

Pennington, T.D., Sarukhán, J., 2005. Árboles tropicales de México. Manual para la identificación de las principales especies. Universidad Nacional Autónoma de México, Mexico.

Piperno, D.R., 1988. Phytolith analysis: an archaeological and geological perspective. Academic Press, San Diego.

Piperno, D.R., 2006. Phytoliths: a comprehensive guide for archaeologists and paleoecologists. AltaMira Press, Lanham, MD.

Piperno, D.R., Pearsall, D.M., 1998. The silica bodies of tropical American grasses: morphology, taxonomy, and implications for grass systematics and fossil phytolith identification. Smithsonian Contribution to Botany, 85,1-40.

Piperno, D.R., Andres, T.C., Stothert, K.E., 2000. Phytoliths in Cucurbita and other Neotropical Cucurbitaceae and their Occurrence in Early Archaeological Sites from the Lowland American Tropics. Journal of Archaeological Science 27, 193–208. https://doi.org/10.1006/jasc.1999.0443

Postek, M.T., 1981. The Occurrence of Silica in the Leaves of Magnolia grandiflora L. Botanical Gazette 142, 124–134. https://doi.org/10.1086/337202

Prat, H., 1948. General Features of the Epidermis in Zea Mays. Annals of the Missouri Botanical Garden 35, 341–351. https://doi.org/10.2307/2394699

Reese-Taylor, K., Mathews, P., Zamora, M., Rangel, M., Walker, D.S., Alvarado, S., Arredondo, E., Morton, S., Parry, R., Salazar, B., and Seibert, J., 2005. Proyecto Arqueológico Naachtun:

Resultados preliminares de la primera temporada de campo 2004. XVIII Simposio de Investigaciones Arqueológicas en Guatemala,85-95.

Rovner, I., 1971. Potential of Opal Phytoliths for use in Paleoecological Reconstruction. Quaternary Research 1, 343–359. https://doi.org/10.1016/0033-5894(71)90070-6

Runge, F., 1999. The opal phytolith inventory of soils in central Africa —quantities, shapes, classification, and spectra. Review of Palaeobotany and Palynology 107, 23–53. https://doi.org/10.1016/S0034-6667(99)00018-4

Sánchez-Sánchez, O., Islebe, G.A., 2002. Tropical forest communities in southeastern Mexico. Plant Ecology 158, 183–200. https://doi.org/10.1023/A:1015509832734

Schultze, M.D., Whitacre, D.F., 1999. A Classification and ordination of the tree community of Tikal National Park. Bulletin of the Florida museum of natural history, 169-297.

Servigne, P., Stevens, R., 2015. Comment tout peut s'effondrer: petit manuel de collapsologie à l'usage des générations présentes. Éditions du Seuil, Paris.

Standley, P.C., Steyermark, J.A., 1946. Flora of Guatemala. Natural History Museum Chicago, Chicago.

Strömberg, C.A.E., 2004. Using phytolith assemblages to reconstruct the origin and spread of grass-dominated habitats in the great plains of North America during the late Eocene to early Miocene. Palaeogeography, Palaeoclimatology, Palaeoecology, Evolution of grass-dominated ecosystems during the late Cenozoic Session at the North American Paleontological Convention, 2001 207, 239–275. https://doi.org/10.1016/j.palaeo.2003.09.028

Strömberg, C.A.E., 2009. Methodological concerns for analysis of phytolith assemblages: Does count size matter? Quaternary International, Perspectives on Phytolith Research: 6th International Meeting on Phytolith Research 193, 124–140. https://doi.org/10.1016/j.quaint.2007.11.008

Tainter, J.A., 1988. The collapse of complex societies, New studies in archaeology. Cambridge University Press, Cambridge, Cambridgeshire ; New York.

Thomas, R., 2011. Anatomie comparée des palmiers: Identification-assistée par ordinateur, Applications en paléobotanique et en archéobotanique. Ph.D. Thesis, Museum national d'Histoire naturelle, Paris.

Thompson, K.M., Hood, A., Cavallaro, D., Lentz, D.L., 2015. Connecting Contemporary Ecology and Ethnobotany to Ancient Plant Use Practices of the Maya at Tikal [WWW Document]. Tikal: Paleoecology of an Ancient Maya City. https://doi.org/10.1017/CBO9781139227209.008

Thorn, V.C., 2004. Phytolith evidence for C4-dominated grassland since the early Holocene at Long Pocket, northeast Queensland, Australia. Quat. res. 61, 168–180. https://doi.org/10.1016/j.yqres.2003.12.002

Tomlinson, P.B., 1961. Anatomy of the monocotyledons, vol. 2: Palmae. Clarendon Press : Oxford University.

Turner, B.L., Sabloff, J.A., 2012. Classic Period collapse of the Central Maya Lowlands: Insights about human-environment relationships for sustainability. Proceedings of the National Academy of Sciences 109, 13908–13914. https://doi.org/10.1073/pnas.1210106109

Twiss, P.C., Suess, E., Smith, R.M., 1969. Morphological Classification of Grass Phytoliths1. Soil Science Society of America Journal 33, 109. https://doi.org/10.2136/sssaj1969.03615995003300010030x

Twiss, P.C., 1992. Predicted World Distribution of C3 and C4 Grass Phytoliths, in: Rapp, G., Mulholland, S.C. (Eds.), Phytolith Systematics: Emerging Issues, Advances in Archaeological and Museum Science. Springer US, Boston, MA, pp. 113–128. https://doi.org/10.1007/978-1-4899-1155-1_6

Wahl, D., Byrne, R., Schreiner, T., Hansen, R., 2006. Holocene vegetation change in the northern Peten and its implications for Maya Prehistory. Quaternary Research 65, 380–389. https://doi.org/10.1016/j.yqres.2005.10.004

Wahl, D., Estrada-Belli, F., Anderson, L., 2013. A 3400 year paleolimnological record of prehispanic human–environment interactions in the Holmul region of the southern Maya lowlands. Palaeogeography, Palaeoclimatology, Palaeoecology 379–380, 17–31. https://doi.org/10.1016/j.palaeo.2013.03.006

Watling, J., Iriarte, J., 2013. Phytoliths from the coastal savannas of French Guiana. Quaternary International, Comprehensive Perspectives on Phytolith Studies in Quaternary Research 287, 162–180. https://doi.org/10.1016/j.quaint.2012.10.030

Watling, J., Iriarte, J., Whitney, B.S., Consuelo, E., Mayle, F., Castro, W., Schaan, D., Feldpausch, T.R., 2016. Differentiation of neotropical ecosystems by modern soil phytolith assemblages and its implications for palaeoenvironmental and archaeological reconstructions II: Southwestern Amazonian forests. Review of Palaeobotany and Palynology 226, 30–43. https://doi.org/10.1016/j.revpalbo.2015.12.002

Wilding, L.P., Drees, L.R., 1973. Scanning Electron Microscopy of Opaque Opaline Forms Isolated from Forest Soils in Ohio1. Soil Science Society of America Journal 37, 647. https://doi.org/10.2136/sssaj1973.03615995003700040047x

Wilson, E.M., 1980. Physical geography of the Yucatan Peninsula. Yucatan: A world apart. University of Alabama Press, Tuscaloosa.

Zurro, D., 2018. One, two, three phytoliths: assessing the minimum phytolith sum for archaeological studies. Archaeol Anthropol Sci 10, 1673–1691. https://doi.org/10.1007/s12520-017-0479-4

Fig. 1. Map of main archaeological sites of the Mayan lowlands and the semi-evergreen tropical forest location. (color)

Fig. 2. Map of plant communities and ecological quadrats location. (color)

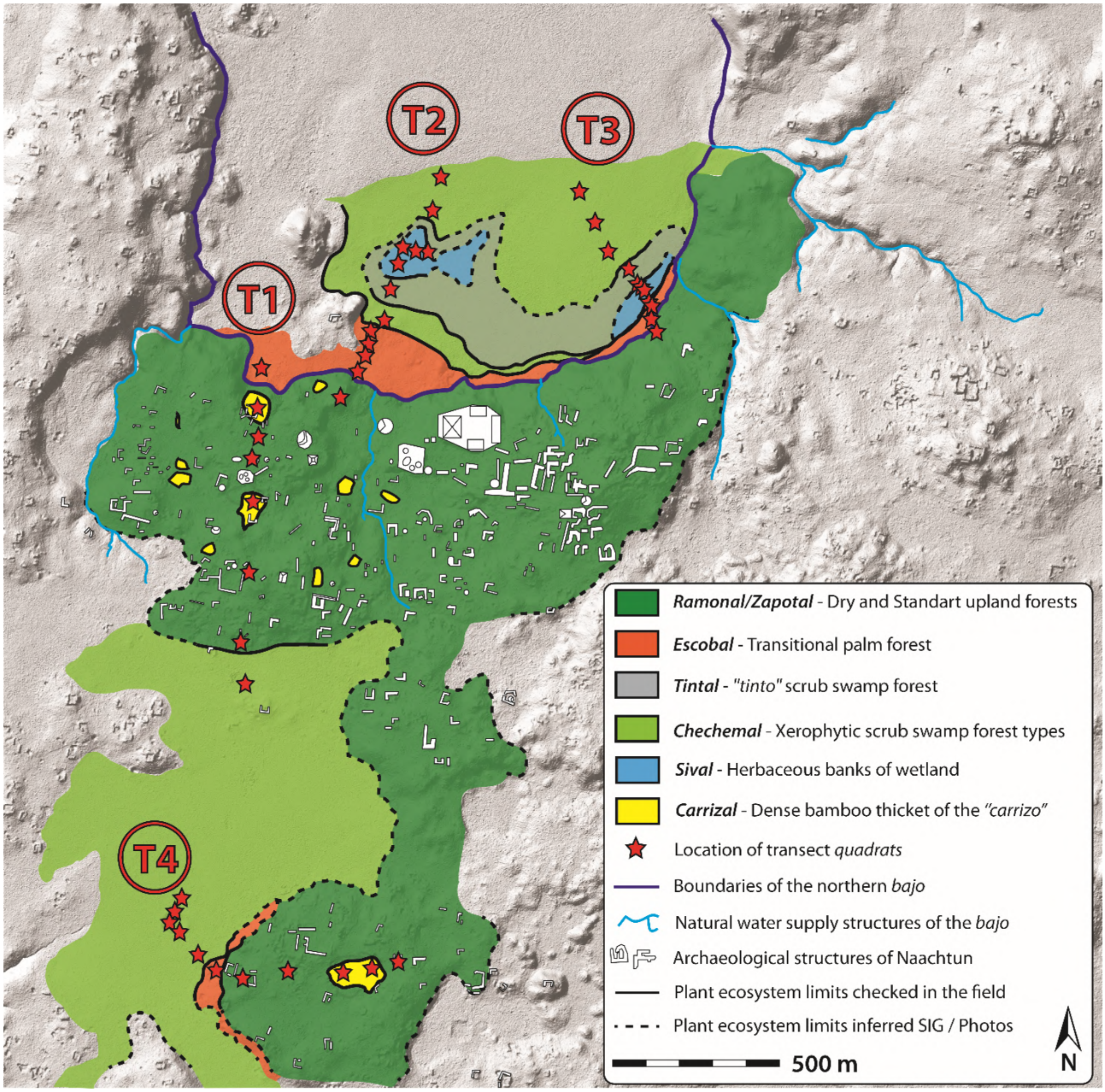

Fig. 3. Ecological transects with plant communities, elevations and quadrat locations. (color)

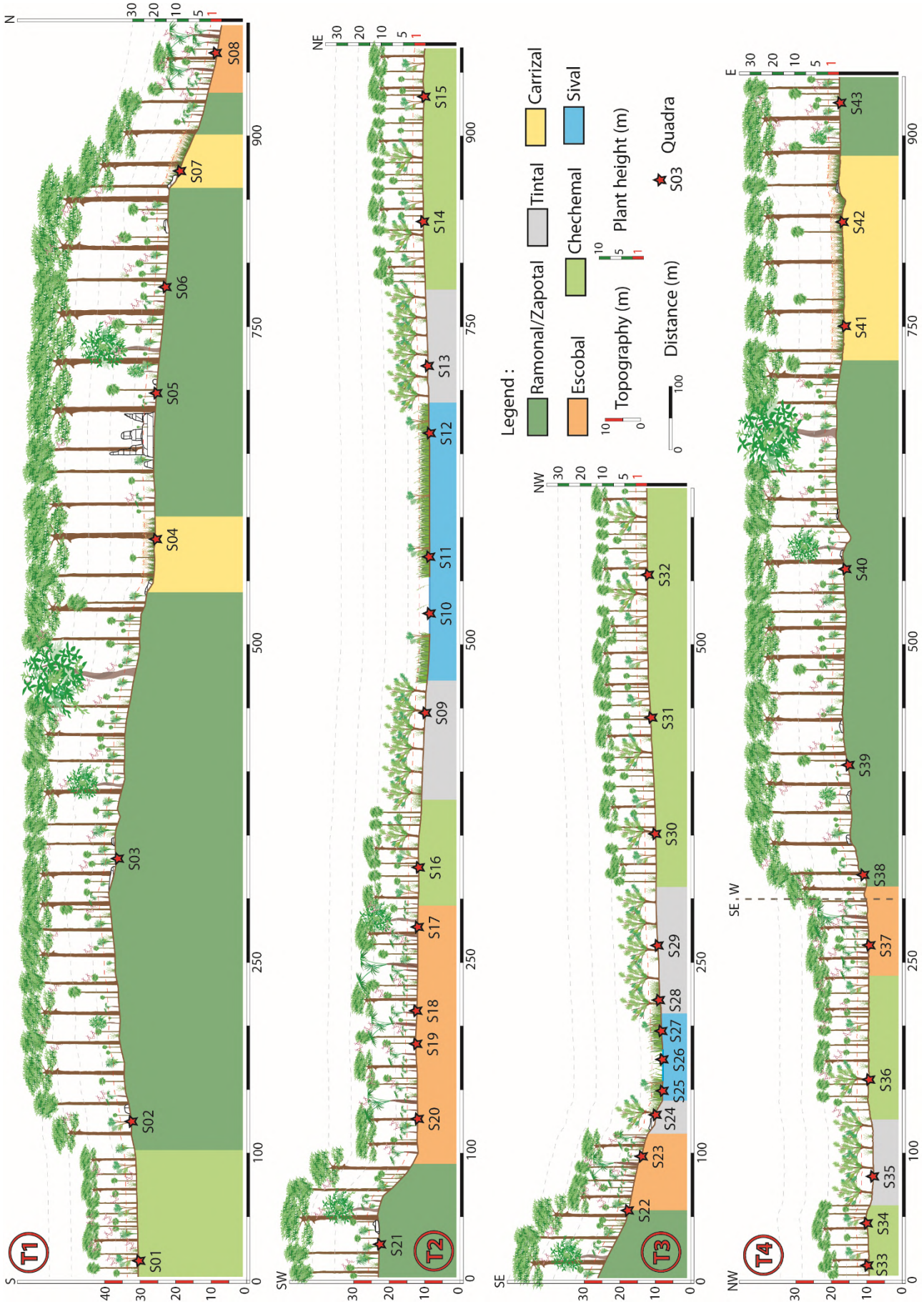

Fig. 4. HAC of plant communities in relation to quadrat species assemblages: Siv = Sival, Tin = Tintal, Che = Chechemal, Ram = Ramonal/Zapotal, Car = Carrizal, Esc = Escobal. (color)

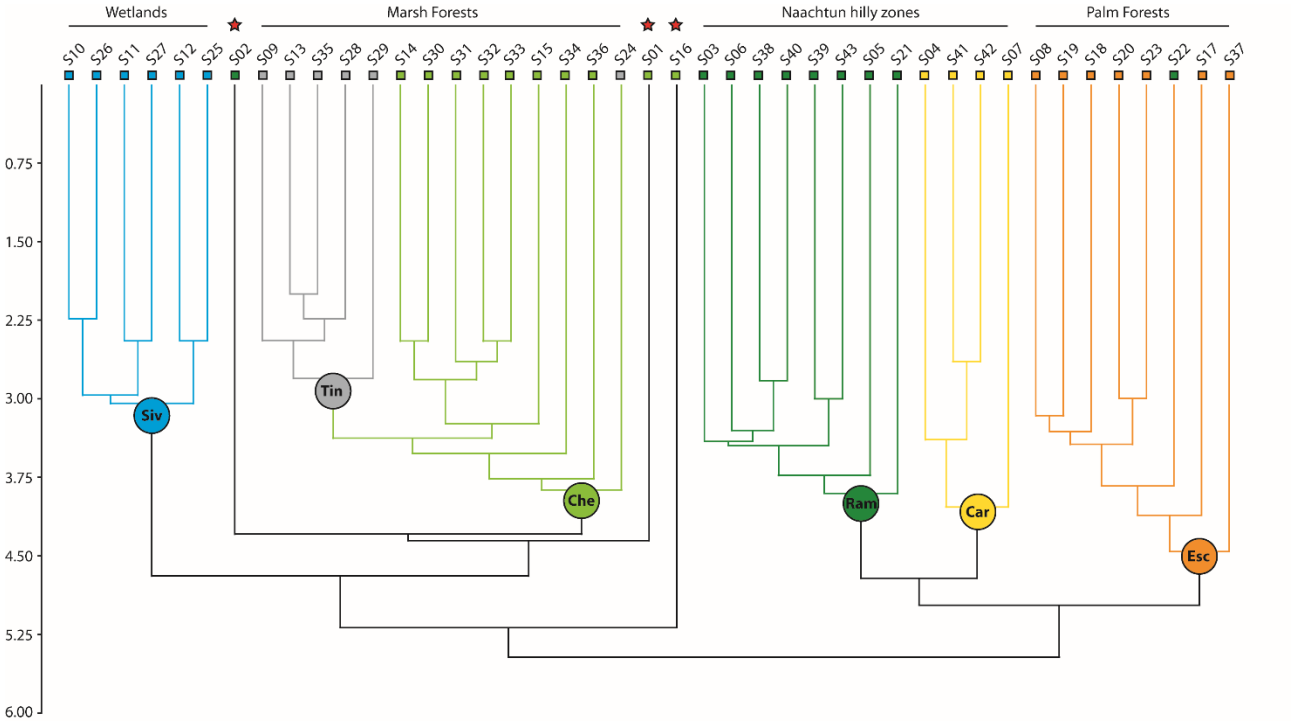

Fig. 5. CA relating to data on the presence of plant species; the plant communities are selected based on HAC. (color)

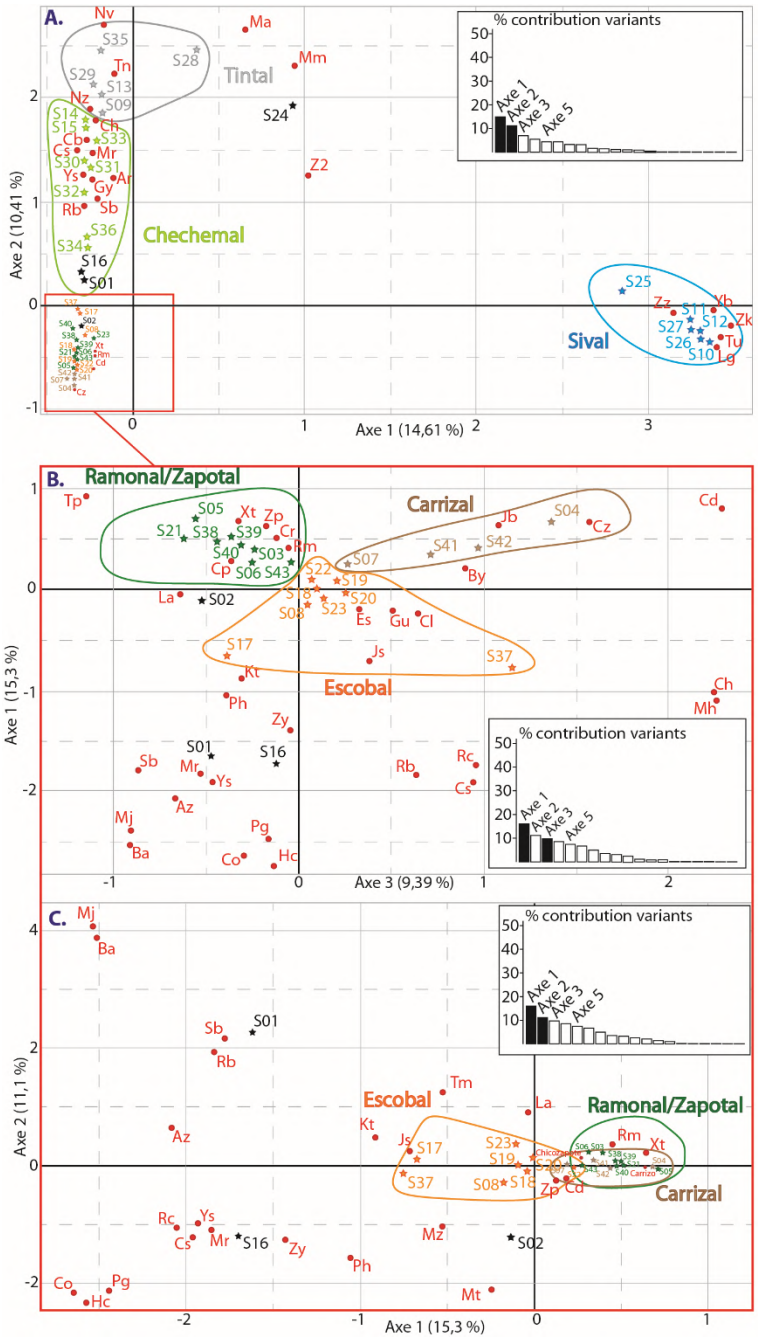

Axe 1

Variab.	Vb.	Cord.	Ctrb.
Zarza	Zz	3,11	24,6 %
Yerba bn.	Yb	3,28	21,1 %
Zakaton	Zk	3,37	17,8 %
Tul	Tu	3,39	13,5 %
Lechuga	Lg	3,41	4,5 %
Arozillo	Az	3,13	3,8 %

Axe 2

Variab.	Vb.	Cord.	Ctrb.
Tinto	Tn	2,18	23,5 %
Chechem N.	Ch	1,78	6,9 %
Cascarillo	Cs	1,37	5,1 %
Navajuel	Nv	2,70	4,0 %
Mozote A.	Ma	2,66	3,9 %
Guayavillo	Gy	1,26	3,5 %
Arozillo	Az	1,25	3,4 %
Yasnic	Ys	1,31	3,3 %
Nanze	Nz	1,83	2,7 %
Mora	Mr	1,39	2,7 %
Roble	Rb	1,09	2.3 %
Caoba	Co	1,50	1,8 %
Zakate II	Z2	1,26	1,7 %
Mozote M.	Mm	2,32	1,5 %
Subin	Sb	1,12	1,4 %
Carrizo	Cz	- 0,80	-1,4 %
Cordoncil.	Cr	- 0,59	- 2,9 %
Ramon	Rm	- 0,61	- 2,8 %
Xate	Xt	- 0,55	- 1,7 %

Axe 1

Variab.	Vb.	Cord.	Ctrb.
Xate	Xt	0,62	4,8 %
Ramon	Rm	0,46	3,7 %
Cordoncil.	Cr	0,38	2,7 %
Carrizo	Cz	0,63	2,0 %
Chicozap.	Cp	0,42	2,0 %
Zapote	Zp	0,37	1,8 %
Palo Horm.	Ph	- 0,99	- 1,9 %
Zikiya	Zy	- 1,40	- 2,8 %
Jiesmo	Js	- 0,70	- 2,5 %
Katsin	Kt	- 0,90	- 3,0 %
Subin	Sb	- 1,78	- 4,0 %
Bejuco aro	Ba	- 2,53	- 4,0 %
Majagua	Mj	- 2,53	- 4,0 %
Mora	Mr	- 1,84	- 4,3 %
Caoba	Co	- 2,64	- 4,4 %
Huev Cab.	Hc	- 2,64	- 4,4 %
Palo Gus.	Pg	- 2,64	- 4,4 %
Cascarillo	Cs	- 1,90	- 4,5 %
Ramon Col.	Rc	- 1,90	- 4,5 %
Arozillo	Az	- 2,07	- 8,0 %

Axe 2

Variab.	Vb.	Cord.	Ctrb.
Carrizo	Cz	1,57	19,8 %
Cedro	Cd	2,27	10,4 %
Bayal	By	0.87	5,4 %
Chechem N.	Ch	2,24	5,1 %
Manchiche	Mh	2,24	5,1 %
Guano	Gn	0,50	4,5 %
Copal	Cl	0,61	4,1 %
Jobillo	Jb	1,09	3,6 %
Cascarillo	Cs	0,99	2,0 %
Ramon Col.	Rc	0,99	2,0 %
Escobo	Es	0,29	1,9 %
Cordoncil.	Cr	- 0,24	- 1,8 %
Xate	Xt	- 0,35	- 2,5 %
Laurel	La	- 0,65	- 2,5 %
Tempisq.	Tp	- 1,13	- 2,6 %

Axe 1

Variab.	Vb.	Cord.	Ctrb.
Xate	Xt	0,62	4,8 %
Ramon	Rm	0,46	3,7 %
Cordoncil.	Cr	0,38	2,7 %
Carrizo	Cz	0,63	2,0 %
Chicozap.	Cp	0,42	2,0 %
Zapote	Zp	0,37	1,8 %
Palo Horm.	Ph	- 0,99	- 1,9 %
Zikiya	Zy	- 1,40	- 2,8 %
Jiesmo	Js	- 0,70	- 2,5 %
Katsin	Kt	- 0,90	- 3,0 %
Subin	Sb	- 1,78	- 4,0 %
Bejuco aro	Ba	- 2,53	- 4,0 %
Majagua	Mj	- 2,53	- 4,0 %
Mora	Mr	- 1,84	- 4,3 %
Caoba	Co	- 2,64	- 4,4 %
Huev Cab.	Hc	- 2,64	- 4,4 %
Palo Gus.	Pg	- 2,64	- 4,4 %
Cascarillo	Cs	- 1,90	- 4,5 %
Ramon Col.	Rc	- 1,90	- 4,5 %
Arozillo	Az	- 2,07	- 8,0 %

Axe 2

Variab.	Vb.	Cord.	Ctrb.
Bejuca aro	Ba	4,14	14,8 %
Majagua	Mj	4,14	14,8 %
Subin	Sb	2,15	8,0 %
Roble	Rb	1,95	6,6 %
Tres marias	Tm	1,28	5,6 %
Laurel	La	0,74	2,8 %
Cascarillo	Cs	- 1,20	- 2,5 %
Ramon Col.	Rc	- 1,20	- 2,5 %
Zikiya	Zy	- 1,30	- 2,9 %
Manzanita	Mz	- 0,99	- 3,4 %
Matapalo	Mt	- 2,04	- 3,6 %
Caoba	Co	- 2,15	- 4,0 %
Huevo Cab.	Hc	- 2,15	- 4,0 %
Palo Gus.	Pg	- 2,15	- 4,0 %
Palo Horm.	Ph	- 1,55	- 6,2 %

1298 Fig. 6. Distribution diagram of phytolith morphotypes. (color)

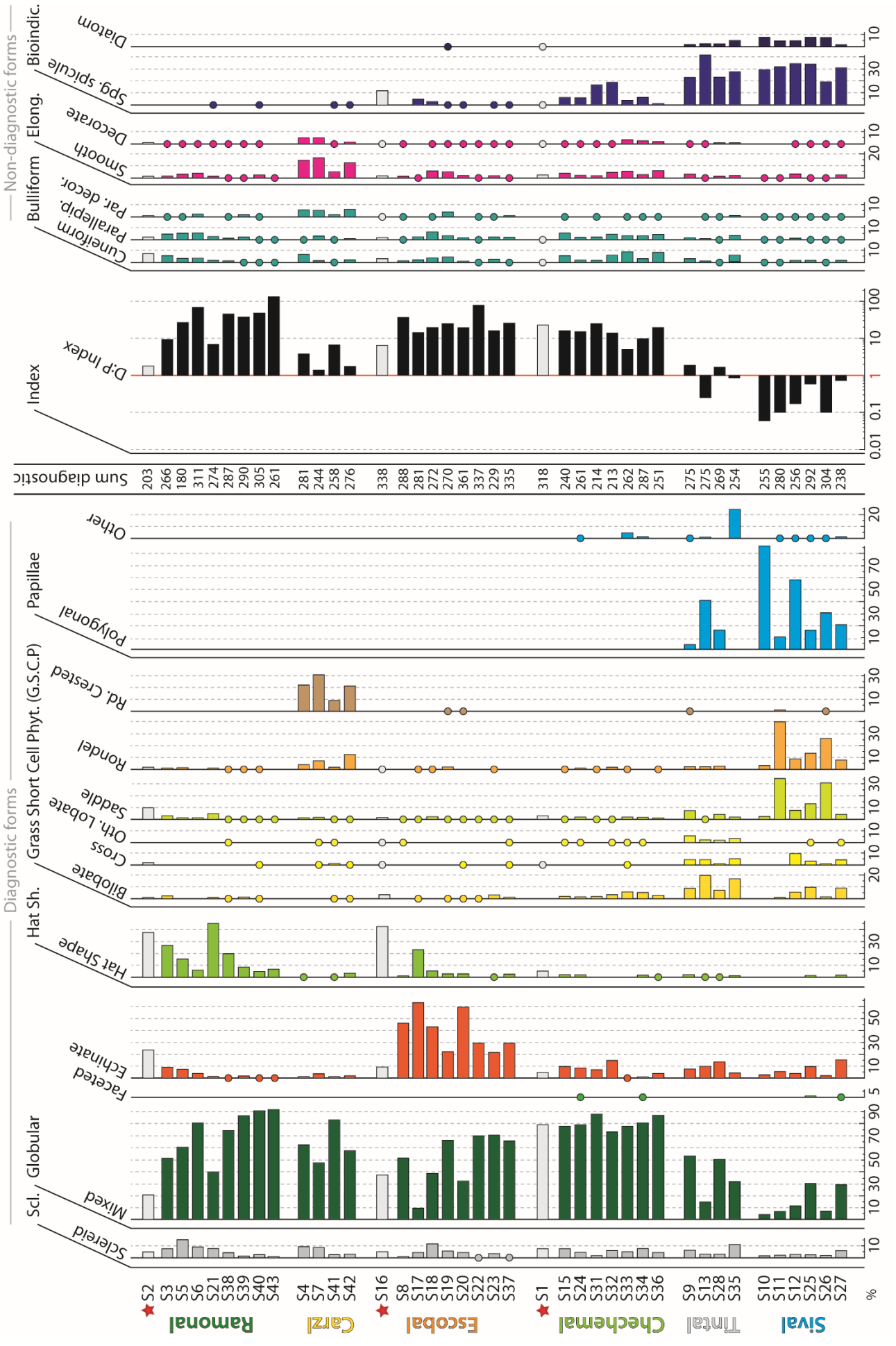
Non-diagnostic forms
Bioindic.
Diatom
Spg. spicule
Elong.
Decorate
Smooth
Bulliform
Par. decor.
Parallelip.
Cuneiform
Index
D:P Index
Sum diagnostic
Diagnostic forms
Papillae
Other
Polygonal
Grass Short Cell Phyt. (G.S.C.P)
Rd. Crested
Rondel
Saddle
Oth. Lobate
Cross
Bilobate
Hat Sh.
Hat Shape
Scl. Globular
Faceted
Echinate
Mixed
Sclereid
%
Siyal
Tintal
Checkemal
Escobal
Carzl
Ramonal
S2 S3 S5 S6 S21 S38 S39 S40 S43
S4 S7 S41 S42
S16 S8 S17 S18 S19 S20 S22 S23 S37
S1 S15 S24 S31 S32 S33 S34 S36
S9 S13 S28 S35
S10 S11 S12 S25 S26 S27

1299

1300 Fig. 7. Statistical distribution of morphotypes by the environments. (color)

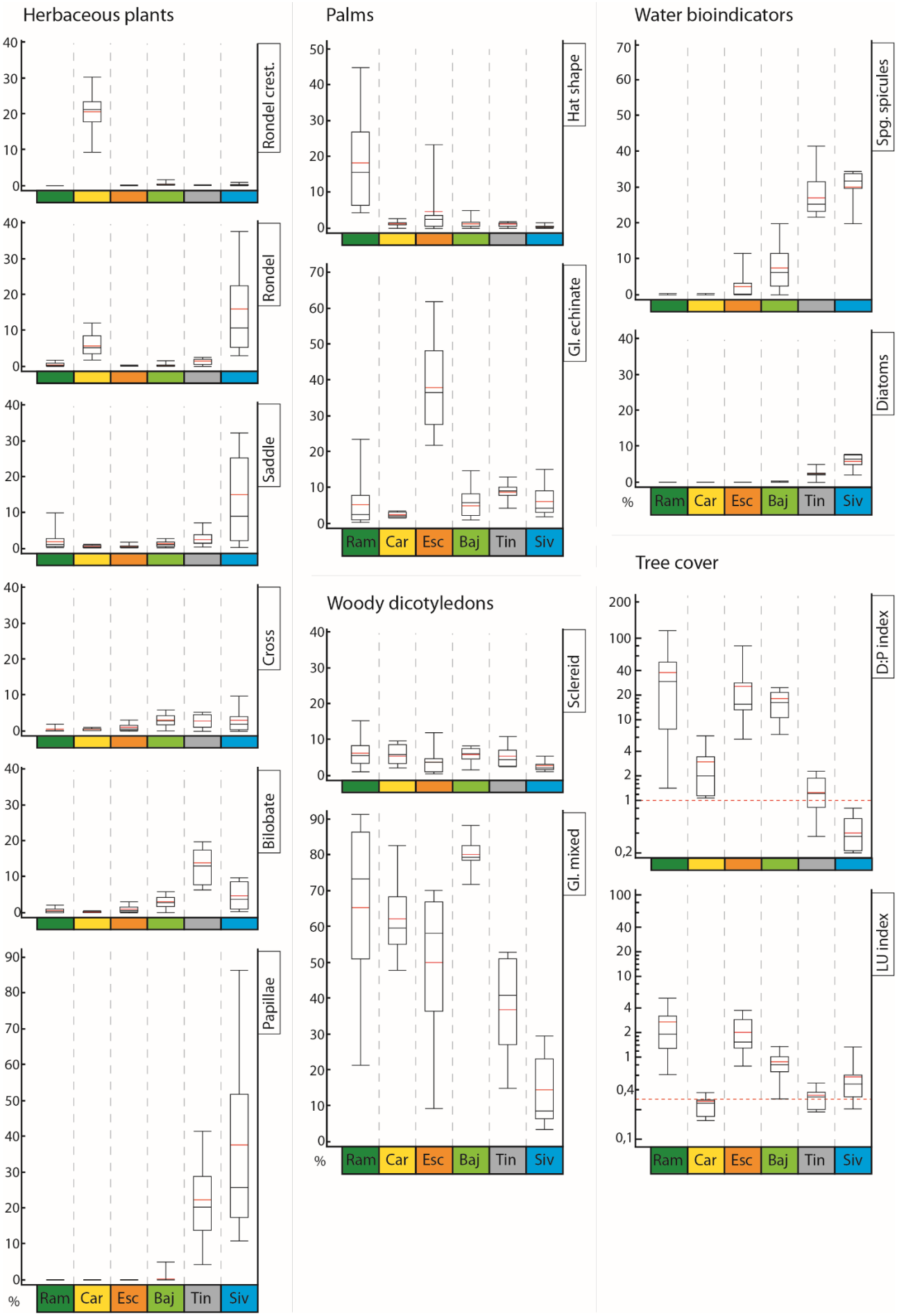

1301

Fig. 8. CA relating to the phytolith distribution diagram. (color)

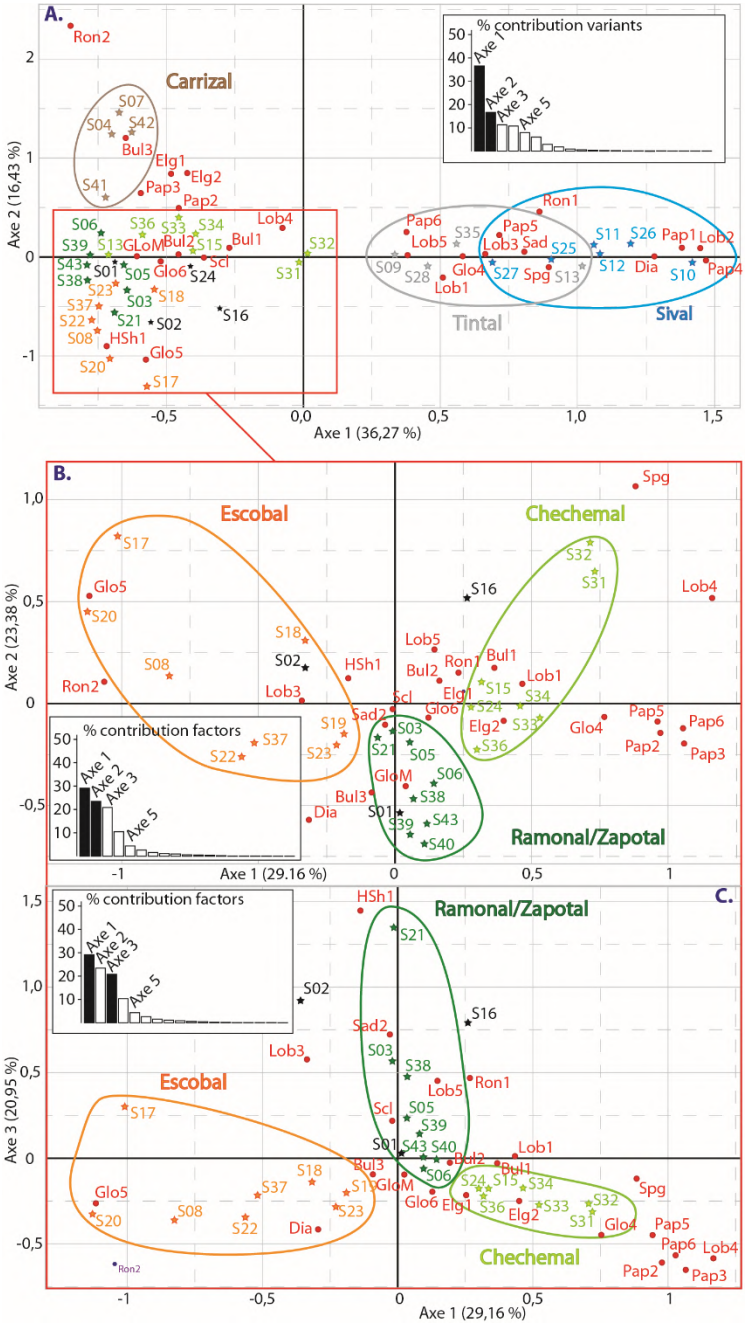

Axe 1

Variab.	Vb.	Crd.	Ctrb.
Sponge spi.	Spg	0,90	31,9 %
Papillae pol.	Pap 4	1,47	16,6 %
Diatom	Dia	1,28	8,4 %
Globular ech.	Glo5	- 0,56	- 4,3 %
Globular mix.	GloM	- 0,62	- 16,6 %

Axe 2

Variab.	Vb.	Crd.	Ctrb.
Rondel crest.	Ron2	2,37	25,5 %
Elongate smt.	Elg1	0,86	15,9 %
Bulliform ech.	Bul3	1,23	9,1 %
Elongate dec.	Elg2	0,87	4,5 %
Hat shape	Hsh1	- 0,90	- 11,5 %
Globular ech.	Glo5	- 1,04	- 31,2 %

Axe 1

Variab.	Vb.	Crd.	Ctrb.
Sponge spi.	Spg	0,90	24,8 %
Globular ech.	Glo5	1,47	- 64,8 %

Axe 2

Variab.	Vb.	Crd.	Ctrb.
Sponge spi.	Spg	1,08	46,6 %
Globular ech.	Glo5	0,49	16,1 %
Globular mix.	GloM	-0,41	- 33,8 %

Axe 1

Variab.	Vb.	Crd.	Ctrb.
Sponge spi.	Spg	0,88	24,8 %
Globular ech.	Glo5	- 1,11	- 64,8 %

Axe 2

Variab.	Vb.	Crd.	Ctrb.
Hat shape	Hsh1	1,44	83,2 %
Globular ech.	Glo5	- 0,26	- 5,0 %

Fig. 9. Evolution of D/P values by environments and quadrats according to the D/P index formulas used (Table 2) and vegetation cover. (color)

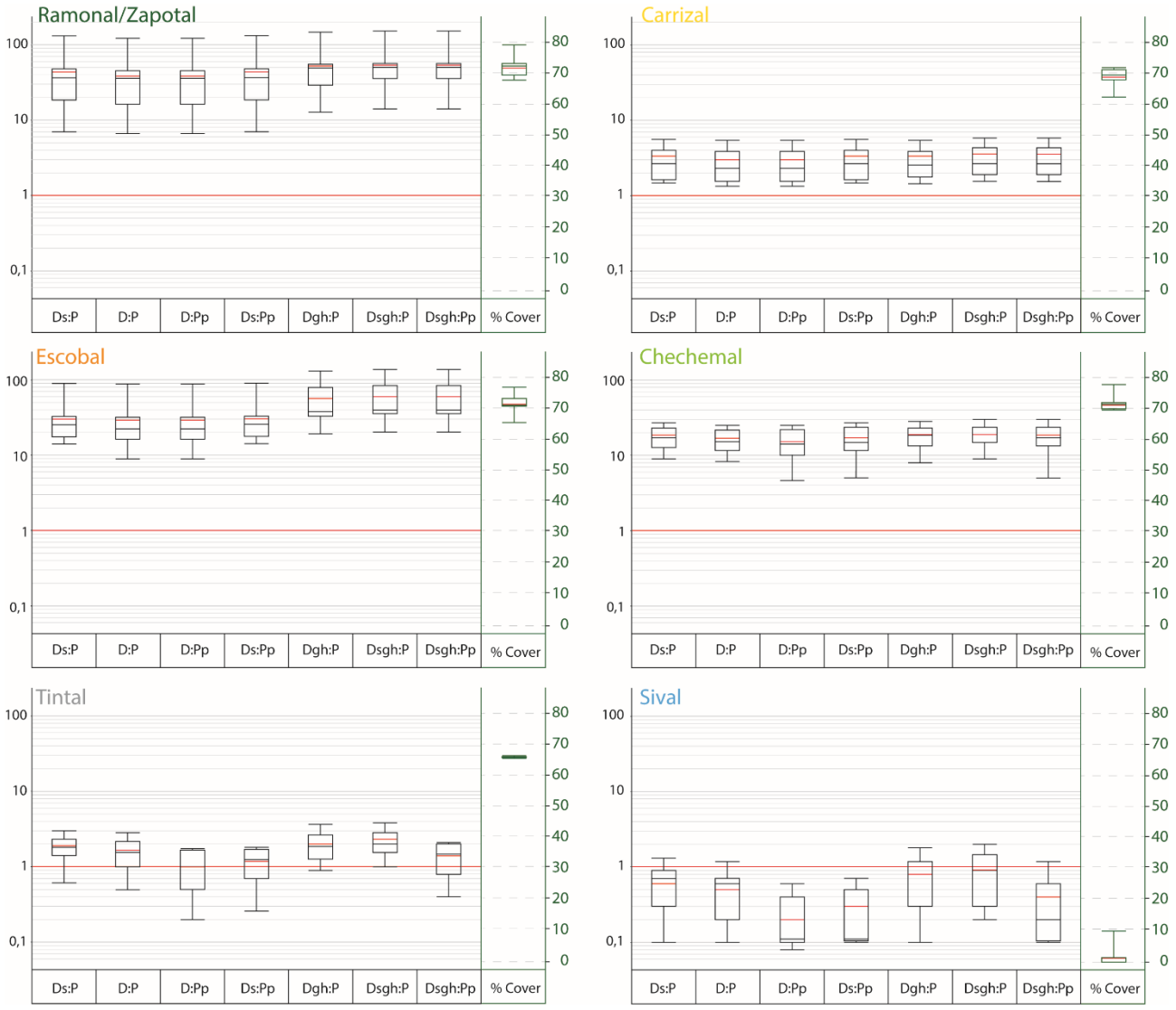

Fig. 10. Evolution of the LU index as a function of the D/P index, the vegetation cover rate and the relative frequency of a grassy undergrowth. (color)

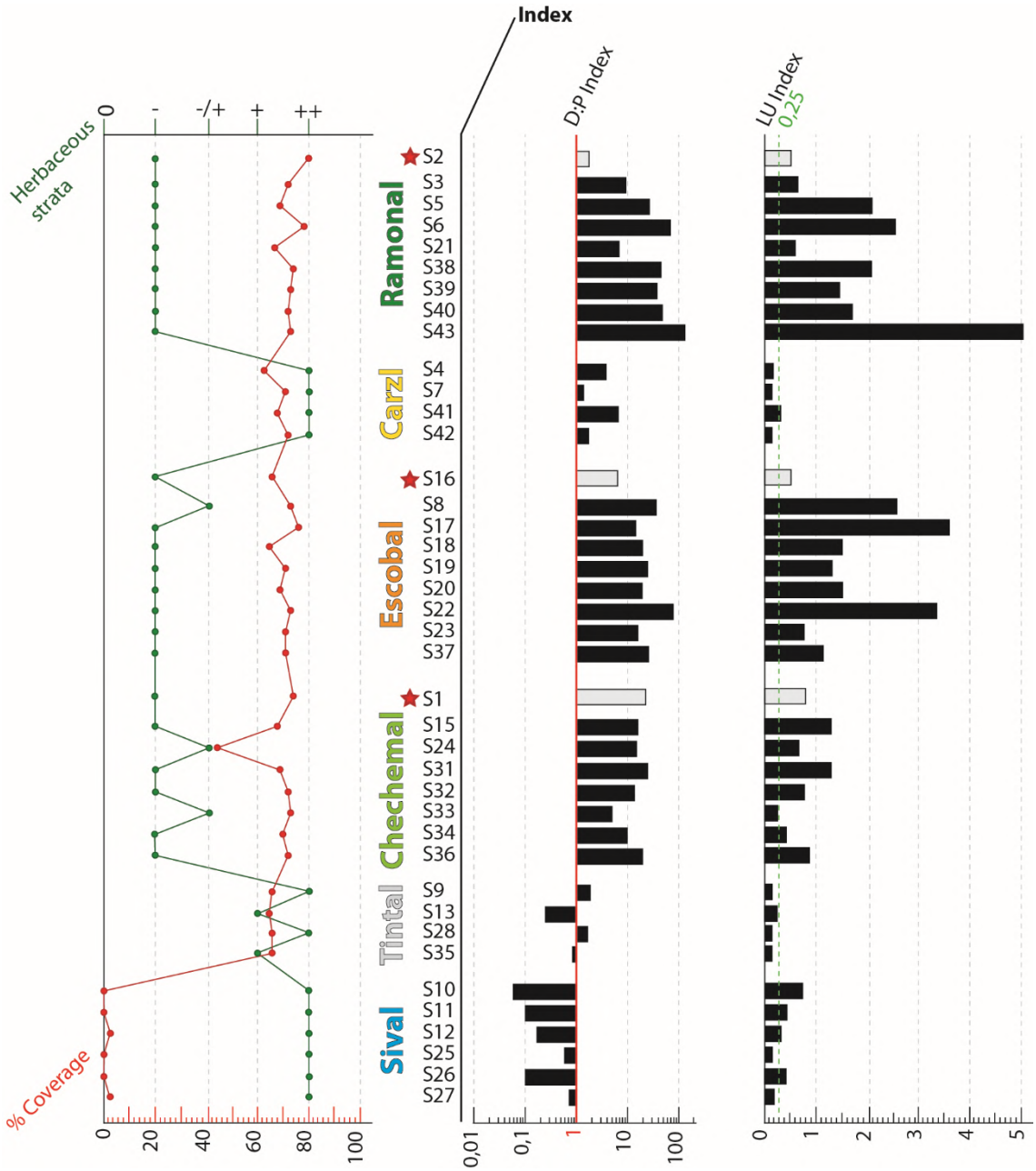

Tab.1: Classification of phytoliths encountered according to the Petén botanical families. Work to observe phytolith morphotypes in current plants: 1. Mulholand, 1989; 2. Ollendorf et al., 1988; 3. Kealhofer & Piperno, 1998; 4. Piperno & Pearsall, 1998b; 5. Thorn, 2004; 6. Lu et al., 2006; 7. Piperno, 2006; 8. Barboni & Bremond, 2009; 9. Honaine et al., 2009; 10. Iriarte & Paz, 2009; 11. Mercader et al., 2009; 12. Eichhorn et al., 2010; 13. Watlling & Iriarte, 2013; 14. Neumann et al. 2017; 15. Collura & Neumann, 2017; 16. Novelo et al. 2018. Classification work of phytolith forms in modern and ancient soils and sediments: 1. Alexandre et al. 1997; 2. Runge, 1999; 3. Stromberg, 2004; 4. Neumann et al., 2009; 5. Garnier et al., 2013; 6. Dickau et al., 2013; 7. Watling et al., 2016. Dicots (Anar. = Anacardiaceae, Apoc. = Apocynaceae, Aral. = Araliaceae, Bign. = Bignoniaceae, Bora. = Boraginaceae, Burs. = Burseraceae, Capp. = Capparaceae, Cele. = Celestraceae, Clus. = Clusiaceae, Euph. = Euphorbiaceae, Faba. = Fabaceae, Laur. = Lauraceae, Malp. = Malpighiaceae, Malv. = Malvaceae, Melia. = Meliaceae, Mora. = Moraceae, Myrt. = Myrtaceae, Picra. = Picramniaceae, Piper. = Piperaceae, Rubi. = Rubiaceae, Sali. = Salicaceae, Sapi. = Sapindaceae, Sapo. = Sapotaceae, Cucu. = Cucurbitaceae, Lamn. = Lamniaceae); Arac. = Araceae; Arec. = Arecaceae (arec. = arecoïdeae, cory. = coryphoïdeae); Cype. = Cyperaceae; Poac. = Poaceae (bamb. = bambusoïdeae, ehrh. = ehrhartoideae, pooï. = pooïdeae, arun. = arundinoïdeae, chlo. = chloridoïdeae, pani. = panicoïdeae).

Cod.	Morphological description	Plt.	Trees																			
			Dicots.	Anar.	Apoc.	Aral.	Bign.	Bora.	Burs.	Capp.	Cele.	Clus.	Euph.	Faba.	Laur.	Malp.	Malv.	Melia.	Mora.	Myrt.	Picra.	Piper.
Pap.1	Plate of 1 to 3 papillae with luminous nucleus (LC)	I ab																				
Pap.2	Smooth irregular shape with short margins and a LC	I ac																				
Pap.3	Smooth irregular shape with elongated LC	I ad																				
Pap.4	Rugulate irregular hexagonal shape with LC	I ae																				
Pap.5	Rugulate irregular shape with collumelated margins with LC	I af																				
Pap.6	Smooth iiregular shape with wavy marges	I ag																				
Lob.1	3D flattened shape, with two lobes connected by a central shank	I m-p																				
Lob.2	Special form of bilobate with the outside of the hollowed lobes																					
Lob.3	3D flattened shape, with 4 lobes connected in a central point	I q-s																				
Lob.4	A special cross shape with only 3 lobes	I t																				
Lob.5	Lengthened lobate shape with at least 3 lobes	I u-v																				
Sad.		I w-x																				
Sad.1	Extended saddle shape with elongated convex sides																					
Sad.2	Saddle shape where convex sides are shorter than concave sides																					
Sad.3	Roughly parallelepiped shape with very high convex margins																					
Sad.4	Non-symmetrical saddle shape with a collapsed plane																					
Ron.																						
Ron.1	Cylindrical shape with opposite bases symmetrical or not	I y-z																				
Ron.2	Rondel shape with a head covered by ridges or thorns in 2D	I aa																				
Scl.		I a-c	4,5,7									3										
Scl.1	Elongated shape, linear or twisted, with facets		5,6				15															
Scl.2	Irregular shape covered by branches in relief		7								16		10									3
Scl.3	Irregular shape covered with pointed ornamentation		2,3,6,7						15										7			
Scl.4	Large irregular shape with smooth size		3,5				15												15			
Scl.5	Smooth polyhedral shape, often in parallelepiped block		4,5				15		3				4	11					15			
Glo.1	Spherical to sub-spherical shape with no visible ornamentation	I e	2,4,5,7	15	3			3	15			13	11	11,13		13			13	10		13
Glo.2	Sub-spherical shape with a rough, warty, or coarse surface	I f-g	1,2,3,4,5,6,7	13					13			14	7	11,13					14	14		13
Glo.3	Spherical to subspherical shapes grouped in the form of a complex	I h	5										3									
Glo.4	Big shape with an ornamented surface by large polygonal faces	I d							2													
Glo.5	Sub-spherical shape with a surface covered by thorns	I i-k																				
Hsh.1	Hemispherical shape covered with thorns	I l																				

	Cod.	Trees Dicots.	Trees Rubi.	Trees Sali.	Trees Sapi.	Trees Sapo.	Herbs Cucu.	Herbs Lamn.	Arac.	Palms Arec.	Palms arec.	Palms cory.	Cype.	Herbs Poac.	Herbs bamb.	Herbs ehrh.	Herbs pooï.	Herbs arun.	Herbs chlo.	Herbs pani.
Papillae	Pap.1												2,5,7,9,13,16							
	Pap.2												2,6,9,13,2							
	Pap.3																			
	Pap.4												2,6,9,10,13,2,4							
	Pap.5																			
	Pap.6																			
Lobate	Lob.1													3	4,8,13,1	8	1,4	1,4,1	1,4,8,1,4	1,4,6,8,13,14,1,4,5,6,7
	Lob.2													3		8,10,14,4,6,7				
	Lob.3													6	4,8,1		1,4	4,1	1,4,8,1	1,4,6,13,14,1,4,5,7
	Lob.4																		8	8,4,5
	Lob.5														7,8		1,4,8	1,8		1,7,8,13,14,5,6,7
Saddle	Sad.														4,6	8	1,5	1,4,4	1,4,8,13,1,6,7	1,4
	Sad.1														10				4,5	
	Sad.2																		4,6,7,14,4,5	
	Sad.3																	4	14	
	Sad.4														6,5					
Rondel	Ron.													4,5,6,7	4,3		1,4,8,3,4,5	1,4,8	1,4,8	1,4,8
	Ron.1													6,7	6		5,6		13	13
	Ron.2																5			
Sclereid	Scl.																			
	Scl.1																			
	Scl.2																			
	Scl.3																			
	Scl.4																			
	Scl.5																			
Globular	Glo.1					15														
	Glo.2																			
	Glo.3						7,11,2,4													
	Glo.4									2,3,4,5,6,7	3,10,13	6,7,10,11								
	Glo.5									2,6,7	7,13									
Hsh.1	Hsh.1																			

Table 2 Different formulas used to calculate the D/P index

Index D:P	Formula
Ds:P	(globular mixed + sclereid)/(GSCP)
D:P	(globular mixed)/(GSCP)
D:Pp	(globular mixed)/(GSCP + papillae)
Ds:Pp	(globular mixed + sclereid)/(GSCP + papillae)
Dgh:P	(globular mixed + globular echinate + hat-shape)/(GSCP)
Dsgh:P	(globular mixed + sclereid + globular echinate + hat-shape)/(GSCP)
Dsgh:Pp	(globular mixed + sclereid + globular echinate + hat-shape)/(GSCP + papillae)

Tab.3 (appendix): Table of correspondence between nomens and scientific names of plant species, relative richness of nomens by plant environments: O : Dominant or typical species of an ecosystem ; +++ : Species observed in at least 75% of the sampling points of an ecosystem ; ++ : Species observed in at least 50% of the sampling points of an ecosystem ; + : Species observed in at least 25% of the sampling points of an ecosystem ; - : Species observed in at least one time of the sampling points of an ecosystem

	Local name	Scientific name	Ram	Car	Esc	Che	Tin	Siv
TREES (> 8 m.)	***Amate***	*Ficus aurea* Nutt.						
		Ficus cotinifolia Kunth				+	-	
		Ficus obtusifolia Kunth						
	Bakelac	*Laetia thamnia* L.	++	++	-			
	Canizte	*Pouteria campechiana* (Kunth) Baehni	+			-		
	Caoba	*Swietenia macrophylla* King				-	-	
	Catalox	*Swartzia cubensis* (Britton & Wilson) Standl.	-					
	Cedro	*Cedrela odorata* L.	-	-				
	Ceibal	*Ceiba pentandra* (L.) Gaertn.				-		
	Chaltecoco	*Caesalpinia velutina* (Britton & Rose) Standl.	+	+		-		
		Caesalpinia violacea (Mill.) Standl.						
	Chechem negro	*Metopium brownei* (Jacq.) Urb.				**O**	-	
	Chicozapote	*Manilkara zapota* (L.) P.Royen	**O**	++	++	++		
	Copal	*Protium copal* (Schltdl. & Cham.) Engl.	++	++	-	-		
	Guaya	*Melicoccus oliviformis* Kunth	++		-	-		
	Huevo de caballo	*Tabernaemontana donnell-smithii* Rose ex J.D.Sm.	-			-		
	Jabin	*Piscidia piscipula* (L.) Sarg.	-		-	++		
	Jobillo	*Astronium graveolens* Jacq.	+					
	Jobo	*Spondias mombin* L.	++	++	+	+		
	K'olo'k	*Talisia floresii* Standl.	+	+	+	-		
	Limonaria	*Trichilia minutiflora* Standl.				-		
	Maculiz	*Tabebuia heterophylla* (DC.) Britton				-		
		Tabebuia rosea (Bertol.) Bertero ex A.DC						
	Madre de Cacao	*Gliricidia sepium* (Jacq.) Walp.				-		
	Malerio blanco	*Aspidosperma megalocarpon* Müll.Arg.	+++	++	++	-		
	Manchiche	*Lonchocarpus castilloi* Standl.	-		-			
	Mano de leon	*Dendropanax arboreus* (L.) Decne. & Planch.	-	-				
	Matapalo	*Clusia flava* Jacq.	-					
	Palo de gusano	*Caesalpinia yucatanensis* Greenm.				-		
		Lonchocarpus guatemalensis Benth.						
	Palo de jiote	*Bursera simaruba* (L.) Sarg.	+	-	-	-		
	Pimienta	*Pimenta dioica* (L.) Merr.	++	++	++	-		
	Ramón	*Brosimum alicastrum* Sw.	**O**	++	++	+		
	Ramón colorado	*Trophis racemosa* (L.) Urb.	-	-	-	-		
	Roble	*Bourreria mollis* Standl.			-	++		
		Ehretia tinifolia L.						
	Siricote	*Cordia dodecandra* A.DC.				-		
	Tempisque	*Sideroxylon floribundum* (Lundell) T.D.Penn.	-					
	Testap	*Guettarda combsii* Urb.	-					
	Tinto	*Haematoxylum campechianum* L.				++	**O**	
	Yasnic	*Vitex gaumeri* Greenm.			+	**O**	-	
	Zapote,	*Manilkara chicle* (Pittier) Gilly						
		Pouteria amygdalina (Standl.) Baehni						
		Pouteria belizensis (Standl.) Cronquist						
		Pouteria durlandii (Standl.) Baehni						
		Pouteria glomerata (Miq.) Radlk.	**O**	++	++	+		
		Pouteria reticulata (Engl.) Eyma						
		Pouteria viridis (Pittier) Cronquist						
		Sideroxylon stevensonii (Standl.) Standl. & Steyerm.						
		Sideroxylon tepicense (Standl.) T.D.Penn.						
SHRUBS	***Arozillo***	ind.				++		
	Cacho de toro	ind.			-	+		

	Cascarillo	*Croton guatemalensis* Lotsy						
		Croton reflexifolius Kunth			-	**O**	-	
	Chaya	*Cnidoscolus aconitifolius* (Mill.) I.M.Johnst.	++	+	++	-		
	Chechem blanco	*Cameraria latifolia* L.			-	+		
	Cordoncillo	*Piper amalago* L.						
		Piper psilorhachis C.DC.	**O**	++	++	-		
	Guayavillo	*Eugenia axillaris* (Sw.) Willd.						
		Eugenia capuli (Schltdl. & Cham.) Hook. & Arn.						
		Eugenia ibarrae Lundell	-			+++		
		Eugenia tikalana Lundell						
	Jiesmo	*Acacia angustissima* (Mill.) Kuntze						
		Acacia dolichostachya S.F.Blake	-	-	-	++		
		Lysiloma acapulcense (Kunth) Benth.						
	Katsin	*Acacia gaumeri* S.F.Blake						
		Acacia riparia Kunth	-	-	-	+		
	Laurel	*Nectandra coriacea* (Sw.) Griseb.						
		Nectandra sanguinea Rol. ex Rottb.	+	-	-	-		
	Majagua	*Hampea tomentosa* (C.Presl) Standl.						
		Hampea trilobata Standl.				++		
		Mortoniodendron guatemalense Standl. & Steyerm.						
	Manzanita	*Malpighia glabra* L.						
		Malpighia lundellii C.V. Morton	-	-		-		
	Mora	*Maclura tinctoria* (L.) D.Don ex Steud.				++	+	
	Nanze	*Byrsonima bucidifolia* Standl.						
		Byrsonima crassifolia (L.) Kunth				+		
	Palo de Hormigas	*Alvaradoa amorphoides* Liebm.	-		-	-		
	Piñón	*Jatropha curcas* L.	-			-		
	Quiebrahacha	*Wimmeria bartlettii* Lundell						
		Wimmeria concolor Cham. & Schltdl.	-					
	Subin	*Acacia collinsii* Saff.						
		Acacia cornigera (L.) Willd.		-	+	+++		
	Zarza	*Mimosa pigra* L.						**O**
	Zikiya	*Chrysophyllum mexicanum* Brandegee						
m. ~		*Chrysophyllum oliviforme* L.			+	-		
PALMS	***Bayal***	*Desmoncus chinantlensis* Liebm. ex Mart.	-	-	+			
	Cambray	*Chamaedorea seifrizii* Burret	++		++	++		
	Escobo	*Cryosophila stauracantha* (Heynh.) R.J.Evans	++		**O**	+		
	Guano / Botan	*Sabal mauritiiformis* (H.Karst.) Griseb. & H.Wendl.	+	+	**O**	+		
		Sabal mexicana Mart.						
	Xate	*Chamaedorea oblongata* Mart.						
		Chamaedorea elegans Mart.	**O**	++	+	+		
	Bejuco de aro	*Bignonia aequinoctialis* L.	-					
	Calabaza de raton	*Cucurbita radicans* Naudin						++
HERBS	***Carrizo***	*Rhipidocladum bartlettii (McClure) McClure*		**O**				
	Lechuga	*Pistia stratiotes* L.						**O**
	Mozote ambra	*Teucrium vesicarium* Mill.						++
	Mozote macho	*Triumfetta semitriloba* Jacq.						++
	Navajuella	Cyperaceae ind.				-	++	+
	Tres marias	*Forchhammeria trifoliata* Radlk. ex Millsp.	-			-		
	Tul'	*Cyperus articulatus* L.						**O**
	Yerba buena	*Mentha × piperita* L.						**O**
	Zakate ambra	*Panicum trichanthum* Nees					++	

Zakate de huecht	*Rhynchospora cephalotes*				+		
Zakate I	*Olyra latifolia L.*	+++	++	++	++	++	
Zakate II	*Kyllinga pumila* Michx.				+		+
Zakate III	*Cyperus ochraceus* Vahl				+		+
Zakate IV	*Leptochloa virgata* (L.) P.Beauv.				-	-	-
Zakaton	*Phragmites australis* (Cav.) Trin. ex Steud.						**O**
Zakaton II	Poaceae ind.						+

Plate I Main morphotypes of diagnostic phytoliths: a-c: sclereid, d: globular faceted, e: globular psilate, f-g: globular decorate, h: globular composed, i-k: globular echinate, l: hat-shape, m-p: bilobate, q-s: cross, t: triangle cross, u-v: polylobate, w-x: saddle, y-z: rondel, aa: rondel crested, ab:

papillae multiple, ac: papillae smooth, ad: papillae long, ae: papillae polygonal, af: papillae collumelate, ag: papillae wavy (color).

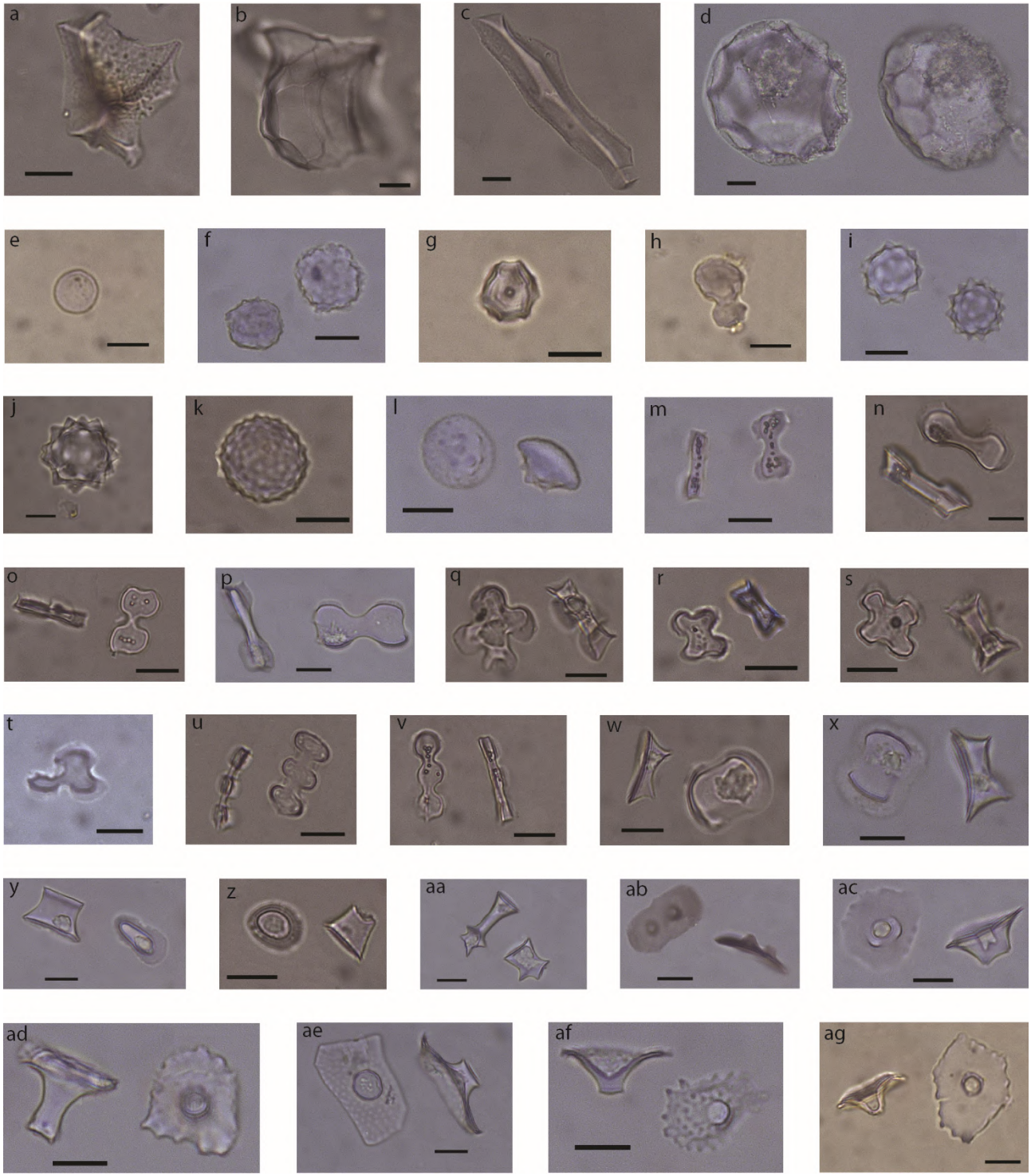

Plate II Main morphotypes of non-diagnostic phytoliths. a-b: bulliform cuneiform, c-d: bulliform psilate, e-f: bulliform decorate, g-h: elongate psilate, i-k: elongate decorate, l-o: sponge spicules, p-s: diatoms. (color)

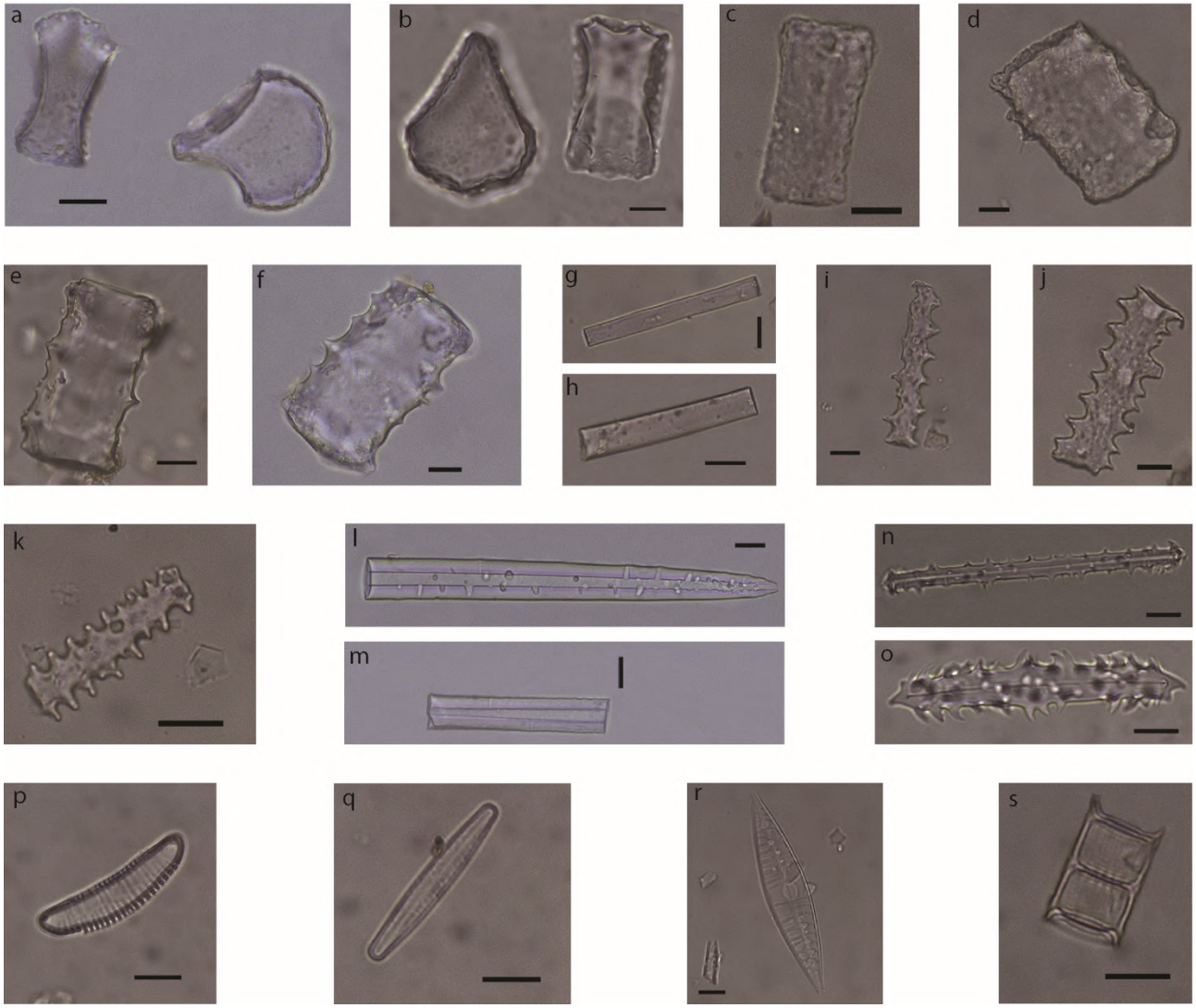

Plate III Plant communities of the Naachtun territory. a: Ramonal/Zapotal, b: Carrizal, c: Escobal, d: Chechemal, e: Tintal, f: Sival. (color)


Ramonal/Zapotal
a.
Carrizal
b.
Escobal
c.
Chechemal
d.
Tintal
e.
Sival
f.

1453